

Mathematics and Mechanics of Solids 0(0): 1–23
©The Author(s) 2013
Reprints and permissions: sagepub.co.uk/journalsPermissions.nav
DOI: 10.1177/1081286513479962
mms.sagepub.com



Active elastodynamic cloaking

Andrew N Norris and Feruza A Amirkulova

Mechanical and Aerospace Engineering, Rutgers University, Piscataway, USA

William J Parnell

School of Mathematics, University of Manchester, Manchester, UK

Received 23 October 2012; accepted 29 January 2013

Abstract

An active elastodynamic cloak destructively interferes with an incident time harmonic in-plane (coupled compressional/shear) elastic wave to produce zero total elastic field over a finite spatial region. A method is described which explicitly predicts the source amplitudes of the active field. For a given number of sources and their positions in two dimensions it is shown that the multipole amplitudes can be expressed as infinite sums of the coefficients of the incident wave decomposed into regular Bessel functions. Importantly, the active field generated by the sources vanishes in the far-field. In practice the infinite summations are clearly required to be truncated and the accuracy of cloaking is studied when the truncation parameter is modified.

Keywords

Active cloaking, elastodynamics, source amplitudes, multipole, Graf's addition theorem

I. Introduction

The main function of a cloaking device is to render an object invisible to some incident wave as seen by some external observer. Over the past decade, a great deal of effort has been focused on passive cloaking, using metamaterials to guide waves around specific regions of space, see e.g. the highly cited works [1–3]. In recent times a rather different approach to cloaking has been noted as an alternative. It has been named active exterior cloaking and it relies on a set of discrete active sources, lying outside the cloaking region, to nullify the incident wave whilst their own radiated field must be negligible in the far-field. Interest has focused on the Helmholtz equation in two dimensions [4–9]. In the work of Vasquez et al. [5,6] Green's formula and addition theorems for Bessel functions were used to formulate an integral equation, which was then converted to a linear system of equations for the unknown amplitudes. Crucially, the integral equation provides the source amplitudes as linear functions of the incident wave field. It was shown that active cloaking can be realized using as few as three active sources in two dimensions (2D). Further work to render the linear relation for the source amplitudes in more explicit form was developed in Vasquez et al. [8] and extended to the three dimensional (3D) Helmholtz case in Vasquez et al. [7]. In Norris et al. [9], the integral representations of Vasquez et al. [8] for the source amplitudes were reduced to closed-form explicit formulas. This obviated the need to reduce the integral equation of Vasquez et al. [5,6] to a system of linear equations which is then required to be solved numerically or to evaluate line integrals, as proposed in Vasquez et al. [8].

Corresponding author:

William J Parnell, School of Mathematics, Alan Turing Building, University of Manchester, Oxford Road, Manchester, M13 9PL, UK. Email: william.parnell@manchester.ac.uk

There is, of course, a strong link between active exterior cloaking and the notion of *anti-sound* or in the context of elastic media, *anti-vibration*. Interestingly the notion of anti-sound appears to have been considered first in a patent published in 1936 by Paul Lueg [10]. The subject has focused greatly on the desire to reduce the magnitude of a radiating field or to create so-called *quiet zones* in enclosed domains such as aircraft cabins using simple sources. The idea to suppress completely the sound field in a finite volume inside an unbounded domain using the Kirchhoff–Helmholtz integral formula and thus employing a continuous distribution of monopoles and dipoles is described in Nelson and Elliott [11]. Anti-vibration techniques have also been developed [12,13]. In general the focus of anti-sound is to reduce the sound radiated from a sound source or to create a zone of silence by employing a finite number of radiating sources. The active field is not required to be non-radiating however. Furthermore, very little work in the anti-sound community has focused on the exact shape of the quiet zone with the exception of David and Elliott [14] who calculated, numerically the zone of silence (<10 dB) region created when the amplitude of a single secondary source was chosen to reduce the noise of a single primary source.

The aim of active exterior cloaking is to render the total field zero inside some prescribed domain (the *cloak* or *zone of silence*), whilst ensuring that the active field itself is non-radiating. The technique introduced in the early active exterior cloaking work enables a cloaked region to be identified clearly by the use of Graf's addition theorem. This approach allows precise determination of the necessary source amplitudes.

The infinite series associated with the multipole expansion of the mth active source is formally divergent inside the circle that is centered on the source itself, i.e. for $|\mathbf{x} - \mathbf{x}_m| < a_m$ in the notation used later on. Therefore the representation for the source is not valid in the domain in which it resides! This point has not been stressed in the active cloaking community, although a related point was noted in the anti-sound community in Kempton [15]. Clearly this point motivates the truncation of the series which has to be done practically in any case. This limits accuracy but as we shall see later in many cases, only a small number of multipoles is required.

As yet it does not appear that active exterior cloaking has been applied to the elastodynamic context. This paper will focus on the relevant 2D active elastodynamic cloaking problem. In general, elastodynamic cloaking problems are more difficult to study than their acoustic or electromagnetic counterparts. Indeed in the case of passive elastodynamic cloaking, this is due to the lack of invariance of Navier's equations under coordinate transformations [16] unless we relax the minor symmetry property of the required elastic modulus tensor. The latter can be achieved by using Cosserat materials [17,18] or by employing non-linear pre-stress of hyperelastic materials [19–21]. Here we show how the active approach to cloaking can be employed in the elastodynamic case for the fully coupled 2D (in-plane) compressional/shear (P/SV) wave problem. As in the approach of Norris et al. [9] we write down the relevant integral equation by employing, in this case, the isotropic Green's tensor. The required source amplitudes for arbitrary wave incidence can be determined explicitly by using Graf's addition theorem.

We shall begin in Section 2 with a statement of the problem, a review of the governing equations, and a summary of the main results. The relevant integral relation is derived in Section 3, from which the main results regarding the explicit form of the source amplitudes are shown to follow. We consider both compressional and transverse (shear) wave incidence. We also describe the form of the active source field and the issues associated with divergence described above. Numerical results follow in Section 4.

2. Problem formulation and main results

2.1. Problem overview

Let us consider the 2D configuration where the active cloaking devices consist of arrays of point multipole sources located at positions $\mathbf{x}_m \in \mathbb{R}^2$, $m = \overline{1, M}$ as depicted in Figure 1. These sources can give rise to both shear and compressional elastic waves. The active sources lie in the exterior region with respect to the cloaked region \mathcal{C} and for this reason, this type of cloaking is called *active exterior cloaking* [5]. Objects are undetectable in the cloaked region by virtue of the destructive interference of the sources and the incident field with the result that the total wave amplitude vanishes in the cloaked region \mathcal{C} . As described in Norris et al. [9] this gives rise to three significant advantages over passive cloaking: (i) the cloaked region is not completely surrounded by a single cloaking device; (ii) only a small number of active sources are needed; (iii) the procedure works for broadband input sources. The principal disadvantage of the method is of course that the incident field must be known.

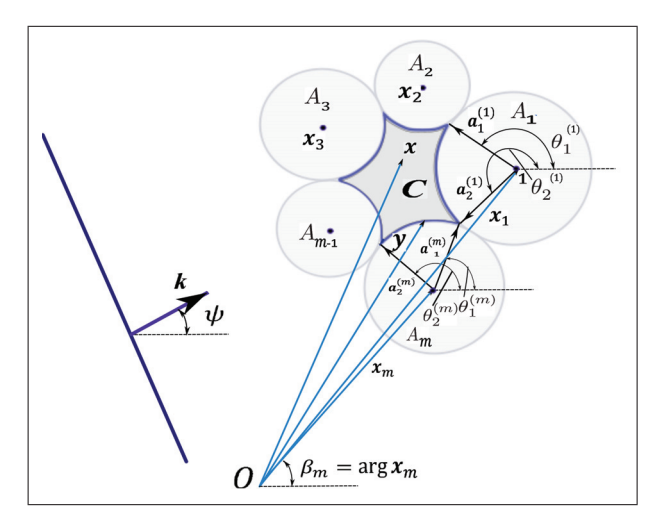


Figure 1. Insonification of the actively cloaked region C generated by M active point multipole sources at \mathbf{x}_m , and active sources regions A_m , $m = \overline{1, M}$. The incident field in this case is a plane wave with wave vector \mathbf{k} in the direction ψ .

The M active sources give rise to a cloaked zone \mathcal{C} as indicated in Figure 1 by the shaded region whose boundary ∂C is the closed concave union of the circular arcs ∂C_m $m = \overline{1, M}$, $\{a_m, \theta_1^{(m)}, \theta_2^{(m)}\}$ associated with the source at \mathbf{x}_m . In the general case $\{a_m, \theta_1^{(m)}, \theta_2^{(m)}\}$ are distinct for different values of m. Note that the wave incidence shown in Figure 1 is a plane wave although the solution derived below is for arbitrary incidence. We therefore have to determine the amplitudes of the active sources as a function of the incident wave, and then prove that the cloaked region is indeed the closed region \mathcal{C} as indicated in Figure 1. Let us also define the notation \mathcal{A}_m as the circular domain of radius a_m that contains the mth active source at its centre. We also define the union of these domains $\mathcal{A} = \bigcup_{m=1}^M \mathcal{A}_m$.

2.2. Compressional/shear (P/SV) in-plane wave propagation

We consider time harmonic solutions with the factor $e^{-i\omega t}$ understood but omitted. Navier's equations in 2D for the displacement $\mathbf{u} = (u_1, u_2), u_j = u_j(x_1, x_2)$, are,

$$\partial_i \sigma_{ij} + \rho \omega^2 u_i = f_i, \quad \sigma_{ij} = C_{ijkl} \, \partial_l u_k,$$
 (1)

where **f** is the forcing, $C_{ijkl} = \lambda \delta_{ij} \delta_{kl} + \mu(\delta_{ik} \delta_{jl} + \delta_{il} \delta_{jk})$ and the summation convention on repeated indices is understood. Hence, in the absence of forcing (**f** = 0),

$$(\lambda + 2\mu)\nabla\nabla \cdot \mathbf{u} + \mu\nabla^2\mathbf{u} + \rho\omega^2\mathbf{u} = 0.$$
 (2)

The Helmholtz decomposition for the displacement,

$$\mathbf{u} = \nabla \Phi + \nabla \times (\Psi \mathbf{k}) \tag{3}$$

leads to separate Helmholtz equations for the scalar potentials

$$\nabla^2 \Phi + k_{\rm p}^2 \Phi = 0, \qquad \nabla^2 \Psi + k_{\rm s}^2 \Psi = 0$$
 (4)

where $k_{\rm p}$, $k_{\rm s}$ are the longitudinal and shear wave numbers, respectively: $k_{\rm p}^2 = \omega^2 \rho/(\lambda + 2\mu)$, $k_{\rm s}^2 = \omega^2 \rho/\mu$. We also define, for later use, $\kappa \equiv k_{\rm s}/k_{\rm p}$, or equivalently $\kappa^2 = 2(1-\nu)/(1-2\nu)$ where ν is Poisson's ratio. We seek the total wave field in the form of an incident wave, \mathbf{u}_i , plus the active source field, \mathbf{u}_d , such that

$$\mathbf{u}(\mathbf{x}) = \mathbf{u}_i + \mathbf{u}_d \quad \Rightarrow \quad \Phi(\mathbf{x}) = \Phi_i + \Phi_d, \qquad \Psi(\mathbf{x}) = \Psi_i + \Psi_d. \tag{5}$$

We assume the general form of an incident field in the regular basis, and hence

$$\begin{pmatrix} \Phi_i \\ \Psi_i \end{pmatrix} = \sum_{n=-\infty}^{\infty} \begin{pmatrix} A_n^{(p)} U_n^+(k_p \mathbf{x}) \\ A_n^{(s)} U_n^+(k_s \mathbf{x}) \end{pmatrix}, \tag{6a}$$

$$\begin{pmatrix} \Phi_d \\ \Psi_d \end{pmatrix} = \sum_{m=1}^{M} \sum_{n=-\infty}^{\infty} \begin{pmatrix} B_{m,n}^{(p)} V_n^+ (k_p(\mathbf{x} - \mathbf{x}_m)) \\ B_{m,n}^{(s)} V_n^+ (k_s(\mathbf{x} - \mathbf{x}_m)) \end{pmatrix}, \tag{6b}$$

where the functions $U_n^{\pm}(\mathbf{z})$ and $V_n^{\pm}(\mathbf{z})$ are defined by

$$U_n^{\pm}(\mathbf{z}) = J_n(|\mathbf{z}|)e^{\pm in\arg\mathbf{z}}, \qquad V_n^{\pm}(\mathbf{z}) = H_n^{(1)}(|\mathbf{z}|)e^{\pm in\arg\mathbf{z}}. \tag{7}$$

Here $\arg \mathbf{z} \in [0, 2\pi)$ and $\arg (-\mathbf{z}) = \arg \mathbf{z} \pm \pi \in [0, 2\pi)$. Define the derivative functions $U_n^{\pm'}(\mathbf{z})$ and $V_n^{\pm'}(\mathbf{z})$ as

$$U_n^{\pm'}(\mathbf{z}) = J_n'(|\mathbf{z}|)e^{\pm in\arg\mathbf{z}}, \qquad V_n^{\pm'}(\mathbf{z}) = H_n^{(1)'}(|\mathbf{z}|)e^{\pm in\arg\mathbf{z}}.$$
 (8)

Note that the functions $U_n^{\pm}(\mathbf{z})$ and $V_n^{\pm}(\mathbf{z})$ possess the properties

$$U_n^{\pm}(-\mathbf{z}) = (-1)^n U_n^{\pm}(\mathbf{z}), \qquad V_n^{\pm}(-\mathbf{z}) = (-1)^n V_n^{\pm}(\mathbf{z}).$$
 (9)

In the following we write U_0 and V_0 , with obvious meaning.

2.3. Summary of the main results

Here we shall state the main results and the required source amplitudes to enable perfect active cloaking together with necessary and sufficient conditions on these amplitudes. The latter ensures we can compare accuracy of the cloaking technique. We shall prove these results in Section 3. Let $\{a_m, \theta_1^{(m)}, \theta_2^{(m)}\}$ define the circular arc ∂C_m of the closed boundary of the cloaked region associated with the source at \mathbf{x}_m . The active source amplitude coefficients for the general form of an incident field (equation (6a)) are

$$\begin{pmatrix}
B_{m,l}^{(p)} \\
B_{m,l}^{(s)}
\end{pmatrix} = \sum_{n=-\infty}^{\infty} \begin{pmatrix}
B_{m,ln}^{(p)} A_n^{(p)} \\
B_{m,ln}^{(s)} A_n^{(s)}
\end{pmatrix}, \text{ where}$$
(10a)

$$\begin{pmatrix} B_{m,ln}^{(p)} \\ B_{m,ln}^{(s)} \end{pmatrix} = \frac{1}{4(k_s a_m)^2} \sum_{q=-\infty}^{\infty} (-1)^q \left[e^{-i(q+l)\theta_2^{(m)}} - e^{-i(q+l)\theta_1^{(m)}} \right]$$

$$\times \left\{ U_{n+q}^{+}(k_{p}\mathbf{x}_{m}) \begin{pmatrix} v_{1}(k_{p}a_{m}, k_{s}a_{m}) \\ v_{2}(k_{p}a_{m}, k_{s}a_{m}) \end{pmatrix} + U_{n+q}^{+}(k_{s}\mathbf{x}_{m}) \begin{pmatrix} -v_{2}(k_{s}a_{m}, k_{p}a_{m}) \\ v_{1}(k_{s}a_{m}, k_{p}a_{m}) \end{pmatrix} \right\}, \tag{10b}$$

$$\mathbf{v}(\alpha,\beta) = \begin{pmatrix} v_1 \\ v_2 \end{pmatrix} = \begin{pmatrix} \left[\frac{\alpha_s^{(m)^2}}{q+l} - 2q\right] \alpha J_l'(\alpha) & i \left[\frac{\alpha_s^{(m)^2}}{q+l} - 2l\right] \alpha J_l(\alpha) \\ -i \left[\alpha_s^{(m)^2} - 2lq\right] J_l(\beta) & -2\alpha_p^{(m)} \alpha_s^{(m)} J_l'(\beta) \end{pmatrix} \begin{pmatrix} J_q(\alpha) \\ iJ_q'(\alpha) \end{pmatrix}.$$
(10c)

The derivation of equation (10) is given in Section 3.4. Alternatively, defining a vector $\mathbf{a}_i^{(m)} \equiv a_m \hat{\mathbf{e}}(\theta_i^{(m)})$ (i = 1, 2), and incorporating equations (7) and (8), equation (10b) reduces to the form

$$\begin{pmatrix}
B_{m,ln}^{(r)} \\
B_{m,ln}^{(s)}
\end{pmatrix} = \frac{1}{4\alpha_s^{(m)^2}} \sum_{q=-\infty}^{\infty} (-1)^q \left\{ U_{n+q}^+(k_p \mathbf{x}_m) \begin{pmatrix} V_1(k_p \mathbf{a}, k_s \mathbf{a}) \\ V_2(k_p \mathbf{a}, k_s \mathbf{a}) \end{pmatrix} + U_{n+q}^+(k_s \mathbf{x}_m) \begin{pmatrix} -V_2(k_s \mathbf{a}, k_p \mathbf{a}) \\ V_1(k_s \mathbf{a}, k_p \mathbf{a}) \end{pmatrix} \right\}_{\mathbf{a}_1^{(m)}}^{\mathbf{a}_2^{(m)}}, \text{ where}$$
(11a)

$$\mathbf{V}(\boldsymbol{\alpha}, \boldsymbol{\beta}) = \begin{pmatrix} V_1 \\ V_2 \end{pmatrix} = \begin{pmatrix} \left[\frac{\alpha_{\rm s}^{(m)^2}}{q+l} - 2q\right] \alpha U_l^{-\prime}(\boldsymbol{\alpha}) & i \left[\frac{\alpha_{\rm s}^{(m)^2}}{q+l} - 2l\right] \alpha U_l^{-}(\boldsymbol{\alpha}) \\ -i \left[\alpha_{\rm s}^{(m)^2} - 2lq\right] U_l^{-}(\boldsymbol{\beta}) & -2\alpha_{\rm p}^{(m)} \alpha_{\rm s}^{(m)} U_l^{-\prime}(\boldsymbol{\beta}) \end{pmatrix} \begin{pmatrix} U_q^{-}(\boldsymbol{\alpha}) \\ i U_q^{-\prime}(\boldsymbol{\alpha}) \end{pmatrix}.$$
(11b)

Next, we note that the active source coefficients $B_{m,l}^{(p)}$ and $B_{m,l}^{(s)}$ must satisfy the necessary and sufficient conditions to ensure active cloaking inside the domain C.

$$\forall n \in \mathbb{Z}: \sum_{m=1}^{M} \sum_{l=-\infty}^{\infty} \times \begin{cases} B_{m,l}^{(p)} U_{n-l}^{-}(k_{p} \mathbf{x}_{m}) &= 0, \\ B_{m,l}^{(s)} U_{n-l}^{-}(k_{s} \mathbf{x}_{m}) &= 0, \end{cases}$$

$$B_{m,l}^{(p)} V_{n-l}^{-}(k_{p} \mathbf{x}_{m}) &= -A_{n}^{(p)},$$

$$B_{m,l}^{(s)} V_{n-l}^{-}(k_{s} \mathbf{x}_{m}) &= -A_{n}^{(s)}.$$

$$(12)$$

The first pair of conditions is required to ensure zero radiated field outside the union of the active regions, \mathcal{A} , and the second pair ensures that the total field is zero inside \mathcal{C} . These constraints on $B_{m,l}^{(p)}$ and $B_{m,l}^{(s)}$ will be used to estimate the error in the active cloaking region in the following sections by truncating the infinite sums in equation (12).

3. Derivation of the source amplitude expressions and constraints

Let us first formulate the problem in terms of an integral equation.

3.1. Green's tensor and integral equation formulation

Consider the particular solution of Navier's equations (1) in the presence of a point force,

$$\mathbf{f} = \mathbf{F}\delta(\mathbf{x} - \mathbf{x}_0) \quad \Rightarrow \quad u_i = G_{ik}F_k \tag{13}$$

where G_{ik} is the 2D (in-plane) Green's tensor. Specifically, $G_{ik}(\mathbf{x})$ satisfies

$$\Sigma_{ijk,j} + \rho \omega^2 G_{ik} = \delta_{ik} \delta(\mathbf{x}), \quad \Sigma_{ijk} = C_{ijpq} G_{pk,q}, \tag{14}$$

with solution

$$G_{ik} = \left(\rho\omega^2\right)^{-1} \left[\delta_{ik} \, k_{\rm s}^2 G_{\rm s} + \partial_i \partial_k (G_{\rm s} - G_{\rm p})\right] \tag{15}$$

where

$$G_{\rm s} = \frac{1}{4i} V_0(k_{\rm s} \mathbf{x}), \qquad G_{\rm p} = \frac{1}{4i} V_0(k_{\rm p} \mathbf{x}).$$
 (16)

The solution in equation (15) can be checked by substitution into the governing equation (14) and using the identities $(\nabla^2 + k_\alpha^2)G_\alpha = \delta(\mathbf{x}), \alpha = \mathbf{p}, \mathbf{s}$.

It is convenient to work without subscripts, writing equation (15) as

$$-\rho\omega^2 \mathbf{G}(\mathbf{x}) = \nabla\nabla G_{\mathbf{p}} + (\mathbf{I}\nabla^2 - \nabla\nabla)G_{\mathbf{s}} = \nabla\nabla G_{\mathbf{p}} + (\nabla\times\mathbf{k})(\nabla\times\mathbf{k})G_{\mathbf{s}} \text{ for } \mathbf{x} \neq 0,$$
(17)

where $(\nabla \times \mathbf{k})_i = e_{ij3} \partial_j$. Using equation (13) in the form $\mathbf{u} = \mathbf{G} \cdot \mathbf{F}$, combined with the Helmholtz decomposition for \mathbf{u} gives

$$\nabla \Phi + (\nabla \times \mathbf{k})\Psi = (\rho \omega^2)^{-1} \left[\nabla \nabla G_p \cdot \mathbf{F} + (\nabla \times \mathbf{k})(\nabla \times \mathbf{k})G_s \cdot \mathbf{F} \right], \quad \mathbf{x} \neq 0, \tag{18}$$

implying

$$-\rho\omega^2\Phi = \mathbf{F} \cdot \nabla G_p = F_1 \partial_1 G_p + F_2 \partial_2 G_p,$$

$$-\rho\omega^2\Psi = \mathbf{F} \cdot (\nabla \times \mathbf{k})G_s = F_1 \partial_2 G_s - F_2 \partial_1 G_s,$$

$$\mathbf{x} \neq 0.$$
(19)

This makes it clear that for a standard point source, regardless of the choice of **F**, both compressional and shear waves propagate away from the point source.

With knowledge of Green's tensor we can now develop an integral equation for the displacement. Indeed, if **u** is a solution of the homogeneous equations in an infinite domain containing a finite region D and σ is the associated stress, then by definition of Green's tensor,

$$\int_{\partial D} dS n_i \left[u_j(\mathbf{y}) \Sigma_{ijk}(\mathbf{y} - \mathbf{x}) - \sigma_{ij}(\mathbf{y}) G_{jk}(\mathbf{y} - \mathbf{x}) \right] = \begin{cases} u_k(\mathbf{x}), & \mathbf{x} \in D, \\ 0, & \mathbf{x} \notin D. \end{cases}$$
(20)

Equation (20) holds for both \mathbf{u}_i and \mathbf{u}_d separately inside the cloaked region, since both are assumed to be regular there (this is a definition of exterior cloaking). Also, by its definition the total field is zero inside the cloaked region with boundary ∂C , and therefore

$$\mathbf{u}_{d}(\mathbf{x}) = -\int_{\partial C} dS \mathbf{n} \cdot \left[\mathbf{u}_{i}(\mathbf{y}) \cdot \mathbf{\Sigma}(\mathbf{y} - \mathbf{x}) - \boldsymbol{\sigma}_{i}(\mathbf{y}) \cdot \mathbf{G}(\mathbf{y} - \mathbf{x}) \right], \quad \mathbf{x} \in C.$$
 (21)

This is the fundamental relation used to find the source amplitudes.

3.2. General expressions for the source amplitudes

Following the procedure for the Helmholtz problem [9], we first substitute the assumed form of \mathbf{u}_d into the left member of equation (21). Then we partition the integral in the right member into M segments over $\{\partial C_m, m = \overline{1, M}\}$ and identify each line integral with the mth component of \mathbf{u}_d , i.e. the part of the source field from the multipoles at \mathbf{x}_m . Thus,

$$0 = \sum_{m=1}^{M} \left\{ \int_{\partial C_m} dS \mathbf{n} \cdot \left[\mathbf{u}_i(\mathbf{y}) \cdot \Sigma(\mathbf{y} - \mathbf{x}) - \sigma_i(\mathbf{y}) \cdot \mathbf{G}(\mathbf{y} - \mathbf{x}) \right] + \sum_{n=-\infty}^{\infty} \left(B_{m,n}^{(p)} \nabla V_n^+(k_p(\mathbf{x} - \mathbf{x}_m)) + B_{m,n}^{(s)} \nabla \times \mathbf{k} V_n^+(k_s(\mathbf{x} - \mathbf{x}_m)) \right) \right\}, \quad \mathbf{x} \in C.$$
(22)

We now use the generalized Graf addition theorem [22, equation (9.1.79)],

$$V_l^+(\mathbf{y} - \mathbf{x}) = \sum_{n = -\infty}^{\infty} \begin{cases} V_n^+(\mathbf{y}) \, U_{n-l}^-(\mathbf{x}), & |\mathbf{y}| > |\mathbf{x}|, \\ U_n^+(\mathbf{y}) \, V_{n-l}^-(\mathbf{x}), & |\mathbf{y}| < |\mathbf{x}|. \end{cases}$$
(23)

The idea is to write $\Sigma(\mathbf{y} - \mathbf{x})$ and $\mathbf{G}(\mathbf{y} - \mathbf{x})$ in equation (22) in terms of sources at \mathbf{x}_m . This suggests using equation (23) for $\mathbf{y} - \mathbf{x} = (\mathbf{y} - \mathbf{x}_m) - (\mathbf{x} - \mathbf{x}_m)$ subject to $|\mathbf{y} - \mathbf{x}_m| < |\mathbf{x} - \mathbf{x}_m|$. Hence, using equation (17),

$$\mathbf{G}(\mathbf{y} - \mathbf{x}) = \frac{i}{4\rho\omega^{2}} \sum_{n=-\infty}^{\infty} \left\{ \nabla \nabla U_{n}^{-} (k_{p}(\mathbf{y} - \mathbf{x}_{m})) V_{n}^{+} (k_{p}(\mathbf{x} - \mathbf{x}_{m})) + (\nabla \times \mathbf{k})(\nabla \times \mathbf{k}) U_{n}^{-} (k_{s}(\mathbf{y} - \mathbf{x}_{m})) V_{n}^{+} (k_{s}(\mathbf{x} - \mathbf{x}_{m})) \right\}.$$
(24)

By virtue of the dependence of Green's function on $\mathbf{y} - \mathbf{x}$, the derivatives $\nabla \nabla$ can be understood as $\nabla_y \nabla_y$ or $\nabla_x \nabla_x$ or $-\nabla_y \nabla_x$, with the same equivalence for $(\nabla \times \mathbf{k})(\nabla \times \mathbf{k})$. Inspection of equation (22) suggests that the forms $-\nabla_y \nabla_x$ and $-(\nabla_y \times \mathbf{k})(\nabla_x \times \mathbf{k})$ are appropriate. Taking into account the negative sign in $\nabla \nabla \to -\nabla_y \nabla_x$, Green's function can be written in the form

$$\mathbf{G}(\mathbf{y} - \mathbf{x}) = \frac{-i}{4\rho\omega^{2}} \sum_{n=-\infty}^{\infty} \left\{ \nabla_{y} U_{n}^{-} (k_{p}(\mathbf{y} - \mathbf{x}_{m})) \nabla_{x} V_{n}^{+} (k_{p}(\mathbf{x} - \mathbf{x}_{m})) + (\nabla_{y} \times \mathbf{k}) U_{n}^{-} (k_{s}(\mathbf{y} - \mathbf{x}_{m})) (\nabla_{x} \times \mathbf{k}) V_{n}^{+} (k_{s}(\mathbf{x} - \mathbf{x}_{m})) \right\}.$$
(25)

Substituting from equation (25) into equation (22), and identifying the coefficients of $\nabla V_n^+(k_p(\mathbf{x} - \mathbf{x}_m))$ and $\nabla \times \mathbf{k} V_n^+(k_s(\mathbf{x} - \mathbf{x}_m))$, yields

$$B_{m,n}^{(p)} = \frac{-i}{4\rho\omega^2} \int_{\partial C_m} dS \mathbf{n} \cdot \left[\boldsymbol{\sigma}_i(\mathbf{y}) \cdot \nabla U_n^- \left(k_p(\mathbf{y} - \mathbf{x}_m) \right) - \mathbf{u}_i(\mathbf{y}) \cdot \sigma^{(p)} \left(k_p(\mathbf{y} - \mathbf{x}_m) \right) \right], \tag{26a}$$

$$B_{m,n}^{(s)} = \frac{-i}{4\rho\omega^2} \int_{\partial C_m} dS \mathbf{n} \cdot \left[\boldsymbol{\sigma}_i(\mathbf{y}) \cdot (\nabla \times \mathbf{k}) U_n^- \left(k_s(\mathbf{y} - \mathbf{x}_m) \right) - \mathbf{u}_i(\mathbf{y}) \cdot \boldsymbol{\sigma}^{(s)} \left(k_s(\mathbf{y} - \mathbf{x}_m) \right) \right], \tag{26b}$$

where

$$\sigma_{ij}^{(p)}(k_{p}(\mathbf{y}-\mathbf{x}_{m})) = C_{ijpq}U_{n,pq}^{-}(k_{p}(\mathbf{y}-\mathbf{x}_{m})),$$

$$\sigma_{ij}^{(s)}(k_{s}(\mathbf{y}-\mathbf{x}_{m})) = C_{ijpq}e_{pr3}U_{n,rq}^{-}(k_{s}(\mathbf{y}-\mathbf{x}_{m})).$$
(26c)

Therefore, given the incident field, we are now able to evaluate the required source amplitudes that guarantee zero total field inside the domain C. We can however, make further progress on the integrals in equation (26) in order to render them in simpler form, by using the fact that ∂C_m is the arc of the circle of radius a_m centered at \mathbf{x}_m , which is the origin of the shifted coordinates $\mathbf{y} - \mathbf{x}_m$. The integration is therefore simplified using polar coordinates centered at \mathbf{x}_m , combined with the expressions for the displacements and traction components in polar coordinates given in terms of the potentials,

$$u_{r} = \Phi_{,r} + \frac{1}{r} \Psi_{,\theta}, \quad u_{\theta} = \frac{1}{r} \Phi_{,\theta} - \Psi_{,r},$$

$$\sigma_{rr} = -\lambda k_{p}^{2} \Phi + 2\mu \left(\Phi_{,rr} + \frac{1}{r} \Psi_{,r\theta} - \frac{1}{r^{2}} \Psi_{,\theta} \right),$$

$$\sigma_{r\theta} = 2\mu \left(\frac{1}{r} \Phi_{,r\theta} - \frac{1}{r^{2}} \Phi_{,\theta} \right) + \mu \left(\frac{1}{r^{2}} \Psi_{,\theta\theta} - \Psi_{,rr} + \frac{1}{r} \Psi_{,r} \right).$$
(27)

The four distinct terms in the integrals of equation (26), such as $dS\mathbf{n} \cdot \boldsymbol{\sigma}_i(\mathbf{y}) \cdot \nabla U_n^-(k_p(\mathbf{y} - \mathbf{x}_m))$, then follow by identifying $\Phi \to U_n^-(k_p\mathbf{a})$, $\Psi \to U_n^-(k_s\mathbf{a})$, where $\mathbf{a}(\theta) \equiv \mathbf{y} - \mathbf{x}_m$ is the radial vector of constant magnitude a_m . Thus,

$$dS\mathbf{n} \cdot \boldsymbol{\sigma}_{i} \cdot \nabla U_{n}^{-} = dS \Big[\sigma_{irr} \frac{\partial}{\partial r} U_{n}^{-} (k_{\mathbf{p}} \mathbf{a}) + \sigma_{ir\theta} \frac{1}{r} \frac{\partial}{\partial \theta} U_{n}^{-} (k_{\mathbf{p}} \mathbf{a}) \Big]$$

$$= d\theta \left(\sigma_{irr} k_{\mathbf{p}} a_{m} U_{n}^{-'} (k_{\mathbf{p}} \mathbf{a}) - i n \sigma_{ir\theta} U_{n}^{-} (k_{\mathbf{p}} \mathbf{a}) \right), \qquad (28a)$$

$$dS\mathbf{n} \cdot \boldsymbol{\sigma}^{(\mathbf{p})} \cdot \mathbf{u}_{i} = dS \Big[u_{ir} \sigma_{rr}^{(\mathbf{p})} + u_{i\theta} \sigma_{r\theta}^{(\mathbf{p})} \Big]$$

$$= d\theta \frac{\mu}{a_{m}} \Big(u_{ir} \Big[(2n^{2} - k_{s}^{2} a_{m}^{2}) U_{n}^{-} (k_{\mathbf{p}} \mathbf{a}) - 2k_{\mathbf{p}} a_{m} U_{n}^{-'} (k_{\mathbf{p}} \mathbf{a}) \Big]$$

$$+ u_{i\theta} 2i n \Big[U_{n}^{-} (k_{\mathbf{p}} \mathbf{a}) - k_{\mathbf{p}} a_{m} U_{n}^{-'} (k_{\mathbf{p}} \mathbf{a}) \Big] \Big), \qquad (28b)$$

$$dS\mathbf{n} \cdot \boldsymbol{\sigma}_{i} \cdot (\nabla \times \mathbf{k}) U_{n}^{-} = dS \Big[\sigma_{irr} \frac{1}{r} \frac{\partial}{\partial \theta} U_{n}^{-} (k_{s} \mathbf{a}) - \sigma_{ir\theta} \frac{\partial}{\partial r} U_{n}^{-} (k_{s} \mathbf{a}) \Big]$$

$$= -d\theta \Big(i n \sigma_{irr} U_{n}^{-} (k_{s} \mathbf{a}) + k_{s} a_{m} \sigma_{ir\theta} U_{n}^{-'} (k_{s} \mathbf{a}) \Big), \qquad (28c)$$

$$dS\mathbf{n} \cdot \boldsymbol{\sigma}^{(s)} \cdot \mathbf{u}_{i} = dS \left[u_{ir} \sigma_{rr}^{(s)} + u_{i\theta} \sigma_{r\theta}^{(s)} \right]$$

$$= d\theta \frac{\mu}{a_{m}} \left(u_{ir} 2in \left[U_{n}^{-}(k_{s}\mathbf{a}) - k_{s} a_{m} U_{n}^{-'}(k_{s}\mathbf{a}) \right] + u_{i\theta} \left[\left((k_{s} a_{m})^{2} - 2n^{2} \right) U_{n}^{-}(k_{s}\mathbf{a}) + 2k_{s} a_{m} U_{n}^{-'}(k_{s}\mathbf{a}) \right) \right). \tag{28d}$$

Noting the reversal of the sense of the integral in equation (26) and incorporating equation (28a) leads to

$$B_{m,l}^{(p)} = \frac{1}{4k_{s}^{2}} \int_{\theta_{1}^{(m)}}^{\theta_{2}^{(m)}} d\theta \, e^{-il\theta} \left\{ i\alpha_{p}^{(m)} J_{l}'(\alpha_{p}^{(m)}) \frac{\sigma_{irr}}{\mu} + lJ_{l}(\alpha_{p}^{(m)}) \frac{\sigma_{ir\theta}}{\mu} + i \left[(\alpha_{s}^{(m)^{2}} - 2l^{2}) J_{l}(\alpha_{p}^{(m)}) + 2\alpha_{p}^{(m)} J_{l}'(\alpha_{p}^{(m)}) \right] \frac{u_{ir}}{a_{m}} + 2l \left[J_{l}(\alpha_{p}^{(m)}) - \alpha_{p}^{(m)} J_{l}'(\alpha_{p}^{(m)}) \right] \frac{u_{i\theta}}{a_{m}} \right\},$$

$$(29a)$$

$$B_{m,l}^{(s)} = \frac{1}{4k_{s}^{2}} \int_{\theta_{1}^{(m)}}^{\theta_{2}^{(m)}} d\theta \, e^{-il\theta} \left\{ -i\alpha_{s}^{(m)} J_{l}'(\alpha_{s}^{(m)}) \frac{\sigma_{ir\theta}}{\mu} + lJ_{l}(\alpha_{s}^{(m)}) \frac{\sigma_{irr}}{\mu} - i \left[(\alpha_{s}^{(m)^{2}} - 2l^{2}) J_{l}(\alpha_{s}^{(m)}) + 2\alpha_{s}^{(m)} J_{l}'(\alpha_{s}^{(m)}) \right] \frac{u_{i\theta}}{a_{m}} + 2l \left[J_{l}(\alpha_{s}^{(m)}) - \alpha_{s}^{(m)} J_{l}'(\alpha_{s}^{(m)}) \right] \frac{u_{ir}}{a_{m}} \right\},$$

$$(29b)$$

where $\alpha_p^{(m)} = k_p a_m$, $\alpha_s^{(m)} = k_s a_m$, $\theta_1^{(m)}$ and $\theta_2^{(m)}$ are the angular positions of the vectors $\mathbf{a}_i^{(m)} \equiv a_m \hat{\mathbf{e}}(\theta_i^{(m)})$, i = 1, 2, which describe the initial and final positions of segment ∂C_m . Equation (29) provides an expression for the source amplitudes for any time harmonic incident field.

Let us now specialize the result to the specific case of plane wave incidence. This is important in its own right but also allows us to derive the general incident wave case by integration as we shall show.

3.3. Plane wave incidence

Let us define

$$u_{\psi_{\alpha}}(\mathbf{x}) = e^{ik_{\alpha}\hat{\mathbf{e}}(\psi_{\alpha})\cdot\mathbf{x}}, \quad \alpha = \mathbf{p}, \mathbf{s}$$
 (30)

where $\hat{\mathbf{e}}(\psi_{\alpha}) = (\cos \psi_{\alpha}, \sin \psi_{\alpha})$ so that $u_{\psi_{\alpha}}$ correspond to compressional (p) and shear (s) plane waves of unit amplitude.

3.3.1. Longitudinal incident plane wave. Consider now longitudinal plane wave incidence

$$\Phi_i(\mathbf{x}) = A_{\mathbf{p}} u_{\psi_{\mathbf{p}}}(\mathbf{x}) \tag{31}$$

where $A_p \equiv const$ is a known wave amplitude. Then using the relation $\Phi_i(\mathbf{y}) = \Phi_i(\mathbf{x}_m)u_{\psi_p}(\mathbf{a})$ with $\mathbf{a} = a_m\hat{\mathbf{e}}(\theta)$, and equation (27) with $\Phi = \Phi_i$, $\Psi = 0$, reduces equation (29) to the form:

$$B_{m,l}^{(p)} = \frac{\Phi_{i}(\mathbf{x}_{m})}{4\kappa\alpha_{s}^{(m)}} \int_{\theta_{1}^{(m)}}^{\theta_{2}^{(m)}} d\theta \ e^{-il\theta} u_{\psi_{p}}(\mathbf{a}) \left\{ i\alpha_{p}^{(m)^{2}} J_{l}'(\alpha_{p}^{(m)}) \left[2\sin^{2}(\theta - \psi_{p}) - \kappa^{2} \right] + l\alpha_{p}^{(m)} J_{l}(\alpha_{p}^{(m)}) \sin 2(\theta - \psi_{p}) - i2l \sin(\theta - \psi_{p}) \left[J_{l}(\alpha_{p}^{(m)}) - \alpha_{p}^{(m)} J_{l}'(\alpha_{p}^{(m)}) \right] - \cos(\theta - \psi_{p}) \left[\left(\alpha_{s}^{(m)^{2}} - 2l^{2} \right) J_{l}(\alpha_{p}^{(m)}) + 2\alpha_{p}^{(m)} J_{l}'(\alpha_{p}^{(m)}) \right] \right\},$$

$$B_{m,l}^{(s)} = \frac{\Phi_{i}(\mathbf{x}_{m})}{4\kappa\alpha_{s}^{(m)}} \int_{\theta_{1}^{(m)}}^{\theta_{2}^{(m)}} d\theta \ e^{-il\theta} u_{\psi_{p}}(\mathbf{a}) \cdot \left\{ \left[2\sin^{2}(\theta - \psi_{p}) - \kappa^{2} \right] l\alpha_{p}^{(m)} J_{l}(\alpha_{s}^{(m)}) - \alpha_{s}^{(m)} J_{l}'(\alpha_{s}^{(m)}) \right] - i\sin 2(\theta - \psi_{p}) \alpha_{p}^{(m)} \alpha_{s}^{(m)} J_{l}'(\alpha_{s}^{(m)}) + i2l \cos(\theta - \psi_{p}) \left[J_{l}(\alpha_{s}^{(m)}) - \alpha_{s}^{(m)} J_{l}'(\alpha_{s}^{(m)}) \right] - \sin(\theta - \psi_{p}) \left[\left(\alpha_{s}^{(m)^{2}} - 2l^{2} \right) J_{l}(\alpha_{s}^{(m)}) + 2\alpha_{s}^{(m)} J_{l}'(\alpha_{s}^{(m)}) \right] \right\}.$$
(32a)

Then noting that $u_{\psi_p}(\mathbf{a}) = e^{ik_p a_m \cos(\theta - \psi_p)} = e^{i\alpha_p^{(m)} \cos(\theta - \psi_p)}$, equation (32) can be written

$$B_{m,l}^{(p)} = \frac{i\Phi_{l}(\mathbf{x}_{m})}{4\kappa\alpha_{s}^{(m)}} e^{-il\psi_{p}} \cdot \left\{ \alpha_{p}^{(m)^{2}} J_{l}'(\alpha_{p}^{(m)}) \left[2L_{0}''(\alpha_{p}^{(m)}) - (\kappa^{2} - 2)L_{0}(\alpha_{p}^{(m)}) \right] - 2l\alpha_{p}^{(m)} J_{l}(\alpha_{p}^{(m)}) L_{1}'(\alpha_{p}^{(m)}) - 2lL_{1}(\alpha_{p}^{(m)}) \left[J_{l}(\alpha_{p}^{(m)}) - \alpha_{p}^{(m)} J_{l}'(\alpha_{p}^{(m)}) \right] + L_{0}'(\alpha_{p}^{(m)}) \left[(\alpha_{s}^{(m)^{2}} - 2l^{2})J_{l}(\alpha_{p}^{(m)}) + 2\alpha_{p}^{(m)} J_{l}'(\alpha_{p}^{(m)}) \right] \right\},$$

$$B_{m,l}^{(s)} = \frac{\Phi_{l}(\mathbf{x}_{m})}{4\kappa\alpha_{s}^{(m)}} e^{-il\psi_{p}} \cdot \left\{ l\alpha_{p}^{(m)} J_{l}(\alpha_{s}^{(m)}) \left[2L_{0}''(\alpha_{p}^{(m)}) - (\kappa^{2} - 2)L_{0}(\alpha_{p}^{(m)}) \right] - 2\alpha_{p}^{(m)} \alpha_{s}^{(m)} J_{l}'(\alpha_{s}^{(m)}) L_{1}'(\alpha_{p}^{(m)}) + 2lL_{0}'(\alpha_{p}^{(m)}) \left[J_{l}(\alpha_{s}^{(m)}) - \alpha_{s}^{(m)} J_{l}'(\alpha_{s}^{(m)}) \right] - L_{1}(\alpha_{p}^{(m)}) \left[(\alpha_{s}^{(m)^{2}} - 2l^{2})J_{l}(\alpha_{s}^{(m)}) + 2\alpha_{s}^{(m)} J_{l}'(\alpha_{s}^{(m)}) \right] \right\},$$

$$(33a)$$

where the functions $L_0(\alpha)$ and $L_1(\alpha)$ are defined by

$$L_{j}(\alpha) = \int_{\theta_{1}^{(m)} - \psi_{p}}^{\theta_{2}^{(m)} - \psi_{p}} d\theta \left(\sin\theta\right)^{j} e^{i(\alpha\cos\theta - l\theta)}, \quad j = 0, 1.$$
(34)

 $L_0(\alpha)$ can be evaluated by using the Jacobi–Anger identity $e^{ix\sin\theta} = \sum_{n=-\infty}^{\infty} J_n(x)e^{in\theta}$,

$$L_{0}(\alpha) = \sum_{n=-\infty}^{\infty} J_{n}(\alpha) i^{n} \int_{\theta_{1}^{(m)} - \psi_{p}}^{\theta_{2}^{(m)} - \psi_{p}} d\theta \, e^{-i(n+l)\theta}$$

$$= \sum_{n=-\infty}^{\infty} J_{n}(\alpha) i^{n+1} \frac{e^{i(n+l)\psi_{p}}}{n+l} \left[e^{-i(n+l)\theta_{2}^{(m)}} - e^{-i(n+l)\theta_{1}^{(m)}} \right]. \tag{35}$$

Integration by parts yields $L_1(\alpha)$ in the form

$$L_1(\alpha) = -\frac{l}{\alpha} L_0(\alpha) - \frac{1}{i\alpha} e^{i(\alpha \cos \theta - l\theta)} \Big|_{\theta_1^{(m)} - \psi_p}^{\theta_2^{(m)} - \psi_p}.$$
(36)

Taking into account the Jacobi–Anger identity and equation (35), the function $L_1(\alpha)$ and its derivative $L'_1(\alpha)$ can be expressed

$$L_1(\alpha) = \frac{1}{\alpha} \sum_{n=-\infty}^{\infty} J_n(\alpha) \, n \, i^{n+1} \, \frac{e^{i(n+l)\psi_p}}{n+l} \cdot \left[e^{-i(n+l)\theta_2^{(m)}} - e^{-i(n+l)\theta_1^{(m)}} \right], \tag{37a}$$

$$L'_{1}(\alpha) = \frac{1}{\alpha^{2}} \sum_{n=-\infty}^{\infty} n \, i^{n+1} \left[\alpha J'_{n}(\alpha) - J_{n}(\alpha) \right] \frac{e^{i(n+l)\psi_{p}}}{n+l} \cdot \left[e^{-i(n+l)\theta_{2}^{(m)}} - e^{-i(n+l)\theta_{1}^{(m)}} \right]. \tag{37b}$$

Introducing the explicit results for the functions $L_0(\alpha)$ and $L_1(\alpha)$ into equation (33) yields expressions for the amplitude coefficients in the form:

$$B_{m,l}^{(p)} = \frac{\Phi_{i}(\mathbf{x}_{m})}{4\kappa^{2}} \sum_{q=-\infty}^{\infty} \frac{i^{q+2}e^{iq\psi_{p}}}{q+l} \cdot \left\{ \alpha_{p}^{(m)}J_{l}'(\alpha_{p}^{(m)}) \left[2J_{l}''(\alpha_{p}^{(m)}) - (\kappa^{2}-2)J_{q}(\alpha_{p}^{(m)}) \right] - \frac{2l\,q}{\alpha_{p}^{(m)}}J_{l}(\alpha_{p}^{(m)}) \left[J_{l}'(\alpha_{p}^{(m)}) - \frac{1}{\alpha_{p}^{(m)}}J_{q}(\alpha_{p}^{(m)}) \right] + J_{l}'(\alpha_{p}^{(m)}) \left[2J_{l}'(\alpha_{p}^{(m)}) + \frac{\alpha_{s}^{(m)^{2}} - 2l^{2}}{\alpha_{p}^{(m)}}J_{l}(\alpha_{p}^{(m)}) \right] - \frac{2l\,q}{\alpha_{p}^{(m)}}J_{q}(\alpha_{p}^{(m)}) \left[\frac{1}{\alpha_{p}^{(m)}}J_{l}(\alpha_{p}^{(m)}) - J_{l}'(\alpha_{p}^{(m)}) \right] \right\}$$

$$\cdot \left[e^{-i(q+l)\theta_{2}^{(m)}} - e^{-i(q+l)\theta_{1}^{(m)}} \right], \qquad (38a)$$

$$B_{m,l}^{(s)} = \frac{\Phi_{i}(\mathbf{x}_{m})}{4\kappa} \sum_{q=-\infty}^{\infty} \frac{i^{q+1}e^{iq\psi_{p}}}{q+l} \cdot \left\{ \frac{l}{\kappa}J_{l}(\alpha_{s}^{(m)}) \left[2J_{l}''(\alpha_{p}^{(m)}) - (\kappa^{2}-2)J_{q}(\alpha_{p}^{(m)}) \right] - 2\,q\,J_{l}'(\alpha_{s}^{(m)}) \left[J_{l}'(\alpha_{p}^{(m)}) - \frac{1}{\alpha_{p}^{(m)}}J_{q}(\alpha_{p}^{(m)}) \right] + 2lJ_{l}'(\alpha_{p}^{(m)}) \left[\frac{1}{\alpha_{s}^{(m)}}J_{l}(\alpha_{s}^{(m)}) - J_{l}'(\alpha_{s}^{(m)}) \right] \right\}$$

$$-J_{l}'(\alpha_{s}^{(m)}) - \frac{q}{\alpha_{p}^{(m)}}J_{q}(\alpha_{p}^{(m)}) \left[\frac{\alpha_{s}^{(m)^{2}} - 2\,l^{2}}{\alpha_{s}^{(m)}}J_{l}(\alpha_{s}^{(m)}) + 2J_{l}'(\alpha_{s}^{(m)}) \right] \right\}$$

$$\cdot \left[e^{-i(q+l)\theta_{2}^{(m)}} - e^{-i(q+l)\theta_{1}^{(m)}} \right]. \qquad (38b)$$

After some simplification equation (38) can be written as

$$\begin{pmatrix}
B_{m,l}^{(p)} \\
B_{m,l}^{(s)}
\end{pmatrix} = \frac{\Phi_{i}(\mathbf{x}_{m})}{4\alpha_{s}^{(m)^{2}}} \sum_{q=-\infty}^{\infty} i^{q} e^{iq\psi_{p}} \cdot \left[e^{-i(q+l)\theta_{2}^{(m)}} - e^{-i(q+l)\theta_{1}^{(m)}} \right] \\
\cdot \begin{pmatrix}
\left[\frac{\alpha_{s}^{(m)^{2}}}{q+l} - 2q \right] \alpha_{p}^{(m)} J'_{l}(\alpha_{p}^{(m)}) & i \left[\frac{\alpha_{s}^{(m)^{2}}}{q+l} - 2l \right] \alpha_{p}^{(m)} J_{l}(\alpha_{p}^{(m)}) \\
-i \left[\alpha_{s}^{(m)^{2}} - 2lq \right] J_{l}(\alpha_{s}^{(m)}) & -2\alpha_{p}^{(m)} \alpha_{s}^{(m)} J'_{l}(\alpha_{s}^{(m)}) \end{pmatrix} \begin{pmatrix}
J_{q}(\alpha_{p}^{(m)}) \\
i J'_{q}(\alpha_{p}^{(m)}) \end{pmatrix}.$$
(39)

3.3.2. Transverse plane wave incidence. Consider now an incident transverse plane wave

$$\Psi_i = A_s e^{ik_s \hat{\mathbf{e}}(\psi_s) \cdot \mathbf{x}},\tag{40}$$

where $A_s \equiv const$ is a known transverse wave amplitude. Entirely analogous calculations to the compressional wave case yield the source amplitudes in the form

$$\begin{pmatrix}
B_{m,l}^{(s)} \\
-B_{m,l}^{(p)}
\end{pmatrix} = \frac{\Psi_{i}(\mathbf{x}_{m})}{4\alpha_{s}^{(m)^{2}}} \sum_{q=-\infty}^{\infty} i^{q} e^{iq\psi_{s}} \left[e^{-i(q+l)\theta_{2}^{(m)}} - e^{-i(q+l)\theta_{1}^{(m)}} \right] \\
\cdot \begin{pmatrix}
\left[\frac{\alpha_{s}^{(m)^{2}}}{q+l} - 2q \right] \alpha_{s}^{(m)} J'_{l}(\alpha_{s}^{(m)}) & i \left[\frac{\alpha_{s}^{(m)^{2}}}{q+l} - 2l \right] \alpha_{s}^{(m)} J_{l}(\alpha_{s}^{(m)}) \\
-i \left[\alpha_{s}^{(m)^{2}} - 2lq \right] J_{l}(\alpha_{p}^{(m)}) & -2\alpha_{p}^{(m)} \alpha_{s}^{(m)} J'_{l}(\alpha_{p}^{(m)}) \end{pmatrix} \begin{pmatrix} J_{q}(\alpha_{s}^{(m)}) \\
i J'_{q}(\alpha_{s}^{(m)}) \end{pmatrix}.$$
(41)

3.3.3. Plane wave incidence summarized. Adding the separate results of equations (39) and (41) gives for combined incidence

$$\Phi_i = A_p e^{ik_p \hat{\mathbf{e}}(\psi_p) \cdot \mathbf{x}}, \quad \Psi_i = A_s e^{ik_s \hat{\mathbf{e}}(\psi_s) \cdot \mathbf{x}}, \tag{42}$$

the source amplitudes

$$\begin{pmatrix}
B_{m,l}^{(p)} \\
B_{m,l}^{(s)}
\end{pmatrix} = \frac{1}{4\alpha_{s}^{(m)^{2}}} \sum_{q=-\infty}^{\infty} i^{q} \left[e^{-i(q+l)\theta_{2}^{(m)}} - e^{-i(q+l)\theta_{1}^{(m)}} \right] \\
\cdot \left\{ \Phi_{i}(\mathbf{x}_{m}) e^{iq\psi_{p}} \begin{pmatrix} v_{1}(\alpha_{p}^{(m)}, \alpha_{s}^{(m)}) \\ v_{2}(\alpha_{p}^{(m)}, \alpha_{s}^{(m)}) \end{pmatrix} + \Psi_{i}(\mathbf{x}_{m}) e^{iq\psi_{s}} \begin{pmatrix} -v_{2}(\alpha_{s}^{(m)}, \alpha_{p}^{(m)}) \\ v_{1}(\alpha_{s}^{(m)}, \alpha_{p}^{(m)}) \end{pmatrix} \right\}$$
(43)

where the vector $\mathbf{v}(\alpha, \beta) = (v_1, v_2)^T$ is defined in equation (10c).

3.4. Arbitrary incident field as superposition of plane incident waves

The general form of incident field given by equation (6a) can be constructed as a superposition of plane incident waves of the form of equation (42). This will enable us to find the general form of the amplitude coefficients for incident waves of general form as a superposition of solutions for plane waves given by equation (43). Recall the incident field for a combined incident plane wave having the form

$$\begin{pmatrix} \Phi_{i}(\mathbf{x}) \\ \Psi_{i}(\mathbf{x}) \end{pmatrix} = \begin{pmatrix} A_{p}e^{ik_{p}\hat{\mathbf{e}}(\psi_{p})\cdot\mathbf{x}} \\ A_{s}e^{ik_{s}\hat{\mathbf{e}}(\psi_{s})\cdot\mathbf{x}} \end{pmatrix} = \sum_{q=-\infty}^{\infty} \begin{pmatrix} i^{q}e^{-iq\psi_{p}}U_{q}^{+}(k_{p}\mathbf{x}) \\ i^{q}e^{-iq\psi_{s}}U_{q}^{+}(k_{s}\mathbf{x}) \end{pmatrix}. \tag{44}$$

Multiplying the first row of equation (44) by $(i^{-(n+q)}/2\pi)e^{i(n+q)\psi_p}$ and the second row by $(i^{-(n+q)}/2\pi)e^{i(n+q)\psi_s}$, integrating with respect to ψ_p and ψ_s respectively between 0 and 2π and then evaluating at $\mathbf{x} = \mathbf{x}_m$ we find

$$\frac{i^{-(n+q)}}{2\pi} \int_{0}^{2\pi} d\psi_{p} \,\Phi_{i}(\mathbf{x}_{m}) e^{i(n+q)\psi_{p}} = U_{n+q}^{+}(k_{p}\mathbf{x}_{m}), \tag{45a}$$

$$\frac{i^{-(n+q)}}{2\pi} \int_0^{2\pi} d\psi_s \, \Psi_i(\mathbf{x}_m) e^{i(n+q)\psi_s} = U_{n+q}^+(k_s \mathbf{x}_m). \tag{45b}$$

To obtain the form of the amplitude coefficients given by equation (10) for the general incidence in equation (6a) we multiply the first and second of the equations in equation (43) by $A_n^{(p)}\gamma_n(\psi_p,\psi_s)$ and $A_n^{(s)}\gamma_n(\psi_p,\psi_s)$ respectively, where $\gamma_n(\psi_p,\psi_s)=i^{-2n}/(2\pi)^2e^{in\psi_p}e^{in\psi_s}$, carry out the double integration with respect to ψ_p and ψ_s between 0 and 2π , incorporate equation (45) and sum over all $n\in\mathbb{Z}$.

3.5. Necessary and sufficient conditions on the source amplitudes

In this section we will define the constraints on the active source coefficients $B_{m,n}^{(p)}$ and $B_{m,n}^{(s)}$ by expressing the active source field \mathbf{u}_d in terms of near-field and far-field source amplitudes and using Graf's addition theorem (equation (23)). When $|\mathbf{x}| > |\mathbf{y}|$ the components of \mathbf{u}_d can be defined as a sum of multipoles at the origin using the first identity in equation (23)

$$\Phi_{d} = \sum_{n=-\infty}^{\infty} F_{n}^{(p)} V_{n}^{+}(k_{p} \mathbf{x}),$$

$$\Phi_{d} = \sum_{n=-\infty}^{\infty} F_{n}^{(s)} V_{n}^{+}(k_{s} \mathbf{x}),$$
for $|\mathbf{x}| > \max(|\mathbf{x}_{m}| + a_{m}),$

$$\Psi_{d} = \sum_{n=-\infty}^{\infty} F_{n}^{(s)} V_{n}^{+}(k_{s} \mathbf{x}),$$
(46)

where

$$F_n^{(p)} = \sum_{m=1}^M \sum_{l=-\infty}^\infty B_{m,l}^{(p)} U_{n-l}^-(k_p \mathbf{x}_m), \quad F_n^{(s)} = \sum_{m=1}^M \sum_{l=-\infty}^\infty B_{m,l}^{(s)} U_{n-l}^-(k_s \mathbf{x}_m). \tag{47}$$

If the active field Φ_d and Ψ_d does not radiate into the far-field, then we must have $F_n^{(p)} = 0$, $F_n^{(s)} = 0$, $\forall n$ ensuring the necessity of equation $(12)_{1,2}$. Sufficiency is guaranteed by substituting the expressions in equation $(12)_{1,2}$ into an assumed far-field of the form of equation (46).

Next we consider the near-field. Assuming $|\mathbf{x}_m| > a_m \ \forall m$ and using the general form of an incident field given by equation (6a), the near-field source amplitudes can be obtained as

$$\Phi_{d} = \sum_{n=-\infty}^{\infty} E_{n}^{(p)} U_{n}^{+}(k_{p} \mathbf{x}),$$

$$\Phi_{d} = \sum_{n=-\infty}^{\infty} E_{n}^{(s)} U_{n}^{+}(k_{s} \mathbf{x}),$$
for $|\mathbf{x}| < \max(|\mathbf{x}_{m}| - a_{m}),$

$$\Psi_{d} = \sum_{n=-\infty}^{\infty} E_{n}^{(s)} U_{n}^{+}(k_{s} \mathbf{x}),$$
(48)

where

$$E_n^{(p)} = \sum_{m=1}^{M} \sum_{l=-\infty}^{\infty} B_{m,l}^{(p)} V_{n-l}^{-}(k_p \mathbf{x}_m), \quad E_n^{(s)} = \sum_{m=1}^{M} \sum_{l=-\infty}^{\infty} B_{m,l}^{(s)} V_{n-l}^{-}(k_s \mathbf{x}_m). \tag{49}$$

If the total field is zero in the near-field, then we must have $E_n^{(p)} + A_n^{(p)}$ and $E_n^{(s)} + A_n^{(s)}$ ensuring the necessity of equation $(12)_{3,4}$. Sufficiency is guaranteed by substituting the expressions in equation $(12)_{3,4}$ into an assumed near-field of the form of equation (48).

3.6. Divergence of the active field summation

The infinite sum expression for the active source fields defined by equation (6b) with source amplitudes (10a)–(10c) is formally valid only in $|\mathbf{x} - \mathbf{x}_m| > a_m$. That is, the expression is not itself valid in the domain \mathcal{A} in which the sources reside! A valid form could be obtained by using the alternative version of Graf's addition theorem in the domain \mathcal{A}_m associated with the arc ∂C_m , but the usual form of Graf in the domain \mathcal{A}_m associated with all other ∂C_n , $n \neq m$. We would then be assured that the active field is zero everywhere outside \mathcal{C} . However if we were to do this, the mth source would not be present in the domain \mathcal{A}_m since the active field would be bounded by construction.

Active cloaking therefore requires that we use the expression in equation (6b) with source amplitudes (10a)–(10c) for the active field everywhere but we must take a finite number of terms in the multipole expansion. That is, we use the source amplitudes that appear in the infinite sum as motivation for the choice of source amplitudes that should be chosen in an active field that contains only a finite number of multipoles. This ensures a finite (but large) field inside A. We should note that this type of difficulty and the fact that it may be used to our advantage in the anti-sound context was noted by Kempton [15].

With a finite sum for the active field therefore, the integral equation (20) is not perfectly satisfied but instead

$$\mathbf{u}(\mathbf{x}) \approx \begin{cases} 0, & \mathbf{x} \in \mathcal{C}, \\ \mathbf{u}_i(\mathbf{x}), & \mathbf{x} \notin \mathcal{C} \cup \mathcal{A}, \end{cases}$$
 (50)

and the field is large (but finite) inside A. Finally we note that a straightforward truncation of the active field may not be optimal in terms of cloaking and ensuring a non-radiating field. This issue will be considered elsewhere.

4. Numerical examples

The numerical calculations for active source configurations of the type shown in Figure 2 are performed for plane longitudinal and transverse incident waves of a unit amplitude, $(A_p = 1, A_s = 0)$ and $(A_p = 0, A_s = 1)$, for angles of incidence $\psi_p = \psi_s = 7^\circ$. Variable values are taken for the wave numbers k_p and k_s , the number of sources M, and the number of terms N in equations (47) and (49) (the truncation size). The M active sources are symmetrically located on a circle of radius b, with

$$a_m = a, \quad |\mathbf{x}_m| = b, \quad \beta_m = (m-1)\beta_0, \quad \beta_0 = 2\pi \left(\frac{m-1}{M}\right), \quad m = \overline{1, M},$$
 (51)

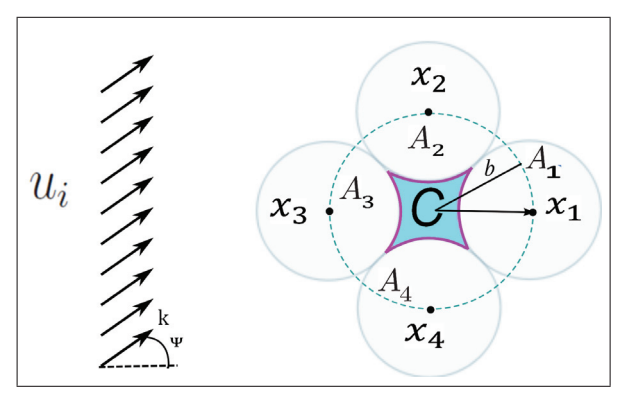


Figure 2. Plane wave insonification of the cloaking region C generated by four (M=4) active sources placed at the corners of a square.

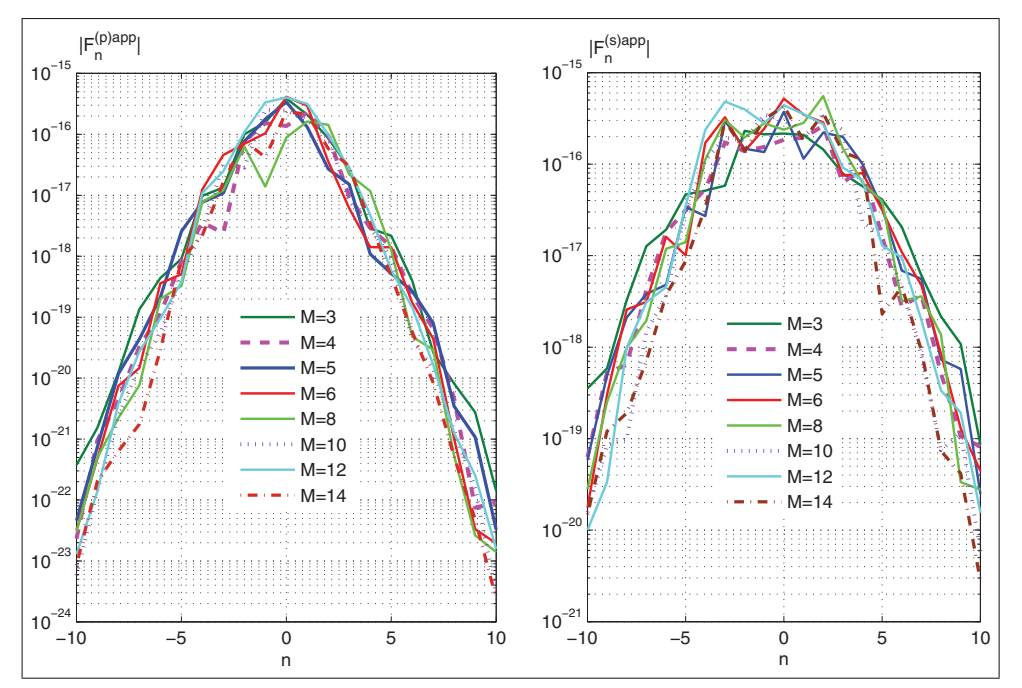


Figure 3. Variation of the far-field amplitude coefficients with number of active sources $(M=\overline{3,14})$ for transverse incident waves. In all cases N=100, $\psi_{\rm S}=7^{\circ}$.

where β_m is the argument of vector \mathbf{x}_m , and $a \geq b \sin \frac{\pi}{M}$. The circular arcs are defined by

$$\theta_{1,2}^{(m)} = \pi + \beta_m \mp \left| \sin^{-1} \left(\frac{b}{a} \sin \frac{\pi}{M} \right) - \frac{\pi}{M} \right|, \quad m = \overline{1, M}.$$
 (52)

In all examples, we take $a=b\sin\frac{\pi}{M}$ and consider an elastic medium having the properties of aluminum with $c_{\rm p}=6427~{\rm m/s},\,c_{\rm s}=3112~{\rm m/s},$ and $\rho=2694~{\rm kg/m^3}$ [23].

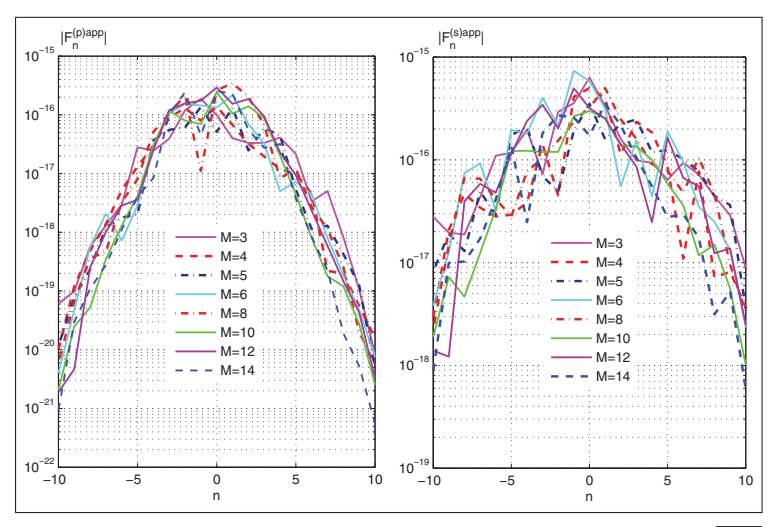


Figure 4. Variation of the far-field amplitude coefficients with number of active sources $(M=\overline{3,14})$ for longitudinal incidence, $N=100, \psi_p=7^\circ$.

4.1. The scattering amplitudes

Consider the truncated versions of the infinite sums in equation (49) for the far-field amplitudes $F_n^{(p)}$ and $F_n^{(s)}$, and equation (47) for the nearfield amplitudes $E_n^{(p)}$ and $E_n^{(s)}$:

$$\frac{F_n^{(\text{p)app}}}{E_n^{(\text{p)app}}} = \sum_{m=1}^M \sum_{l=-N}^N B_{m,l}^{(\text{p})} \times \begin{cases} U_{n-l}^-(\mathbf{x}_m), \\ V_{n-l}^-(\mathbf{x}_m), \end{cases} \quad \forall n \in \mathbb{Z},$$
(53a)

$$\begin{bmatrix}
F_n^{(s)app} \\
E_n^{(s)app}
\end{bmatrix} = \sum_{m=1}^M \sum_{l=-N}^N B_{m,l}^{(s)} \times \begin{cases}
U_{n-l}^-(\mathbf{X}_m), \\
V_{n-l}^-(\mathbf{X}_m),
\end{cases} \quad \forall n \in \mathbb{Z}.$$
(53b)

The approximate near-field $E_n^{(p)app}$, $E_n^{(s)app}$ and far-field $F_n^{(p)app}$, $F_n^{(s)app}$ amplitudes are calculated at the incident shear wave number $k_s=5$ varying the number of active sources M and the truncation size N. The dependence of the far-field coefficients $|F_n^{(p)app}|$, $|F_n^{(s)app}|$ is illustrated in Figure 3 for transverse and in Figure 4 for longitudinal wave incidences. As M increases, the far-field coefficients fluctuate at small |n|, and decrease at larger values of |n| for both compressional and shear incident waves.

The variation of the near-field coefficients $|A_n^{(p)} + E_n^{(p)app}|$, $|A_n^{(s)} + E_n^{(s)app}|$ with the number of sources M is depicted in Figure 5 for transverse and in Figure 6 for longitudinal incident waves. For longitudinal wave incidence, the near-field $|A_n^{(p)} + E_n^{(p)app}|$ is less than 10^{-4} and $|A_n^{(s)} + E_n^{(s)app}|$ is less than 10^{-7} . In contrast, the results are less accurate for transverse waves, as the near-field $|A_n^{(p)} + E_n^{(p)app}|$ approaches the order of 10^{-1} and $|A_n^{(s)} + E_n^{(s)app}|$ reaches a value 10^{-4} .

Figure 7 displays the near-field amplitude coefficients $|A_n^{(p)} + E_n^{(p)app}|$ and $|A_n^{(s)} + E_n^{(s)app}|$ as functions of n, the order of Bessel function, for different values of N and M. The accuracy of the near-field coefficients improves as N and M increase. Increasing the number of sources M allows a decrease in the truncation size N and the order of error.

4.2. Far-field response

The radiated field as $\mathbf{x} \to \infty$ is given by equation (46). Using the asymptotic expansion of the Hankel function for large argument yields the far-field behavior of \mathbf{u}_d

$$\Phi_d = f^{(p)}(\theta) \frac{e^{ik_p|\mathbf{x}|}}{\sqrt{k_p|\mathbf{x}|}} \left[1 + O\left(\frac{1}{k_p|\mathbf{x}|}\right) \right], \quad \Psi_d = f^{(s)}(\theta) \frac{e^{ik_s|\mathbf{x}|}}{\sqrt{k_s|\mathbf{x}|}} \left[1 + O\left(\frac{1}{k_s|\mathbf{x}|}\right) \right], \tag{54}$$

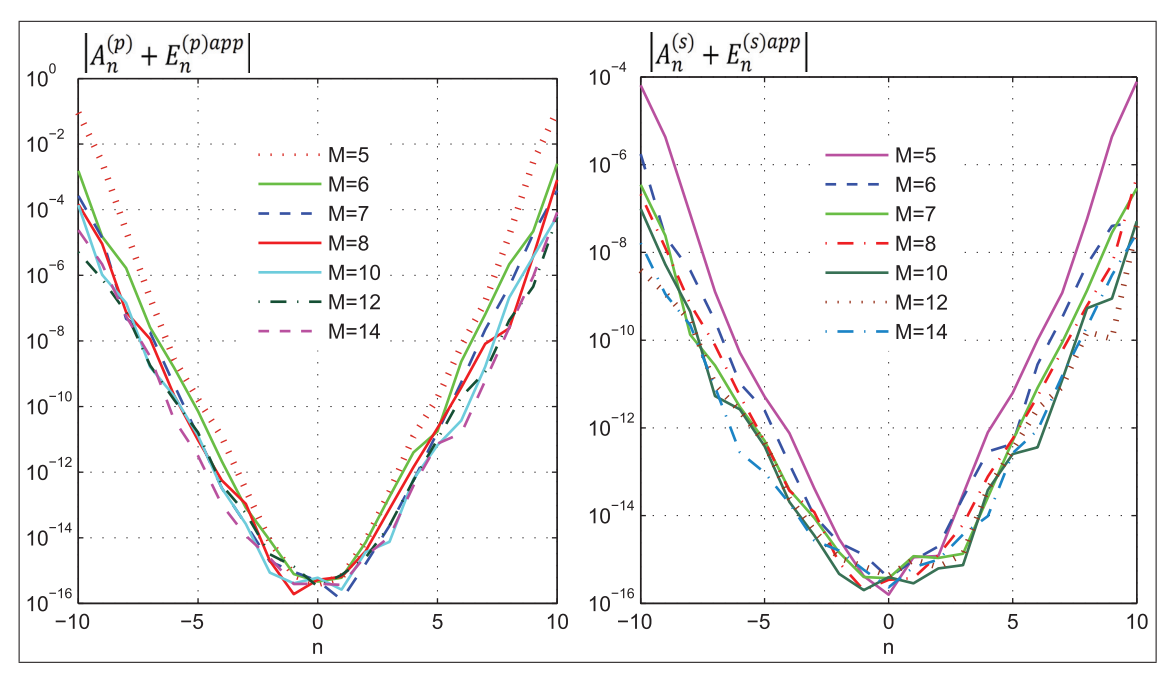


Figure 5. Dependence of the near-field amplitude coefficients on n, the order of Bessel function, varying the number of active sources $(M = \overline{5,14})$ for transverse incidence, N = 100, $\psi_{\rm S} = 7^{\circ}$.

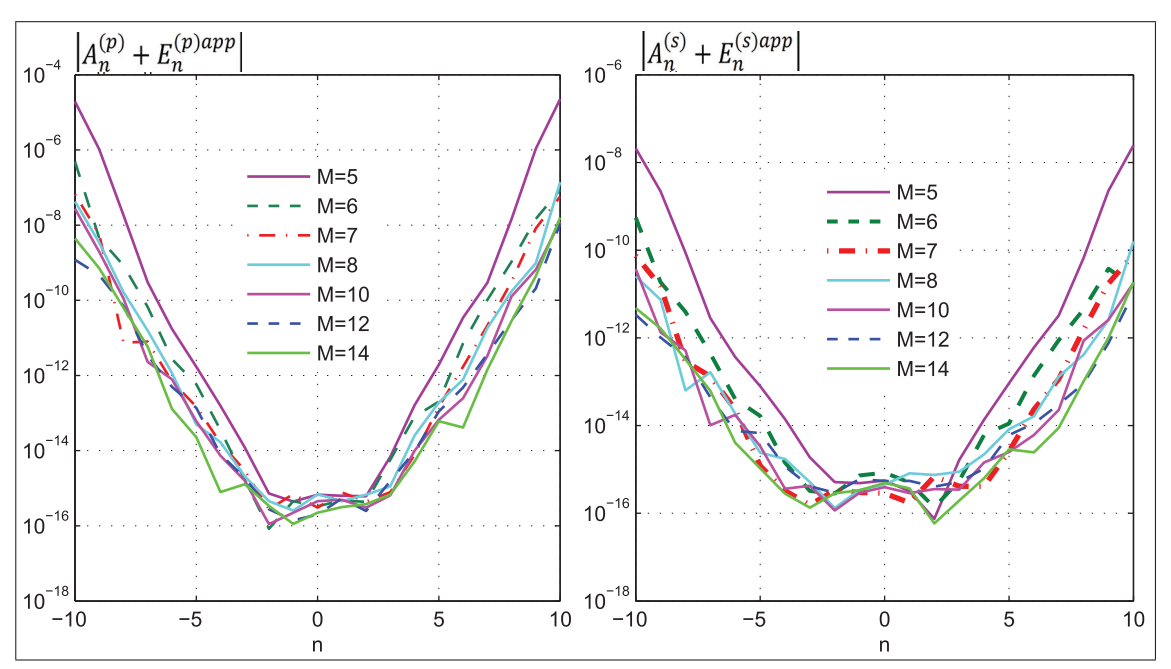


Figure 6. Variation of the near-field amplitude coefficients with number of active sources $(M=\overline{5,14})$ for longitudinal wave incidence, $N=100,\,\psi_{\rm p}=7^{\circ}.$

where $f^{(p)}$ and $f^{(s)}$ are the far-field amplitude functions,

$$f^{(\alpha)}(\theta) = \sum_{n = -\infty}^{\infty} f_n^{(\alpha)} e^{in\theta}, \quad f_n^{(\alpha)} = (-i)^n e^{-i\frac{\pi}{4}} \sqrt{\frac{2}{\pi}} F_n^{(\alpha)}, \quad \alpha = p, s.$$
 (55a)

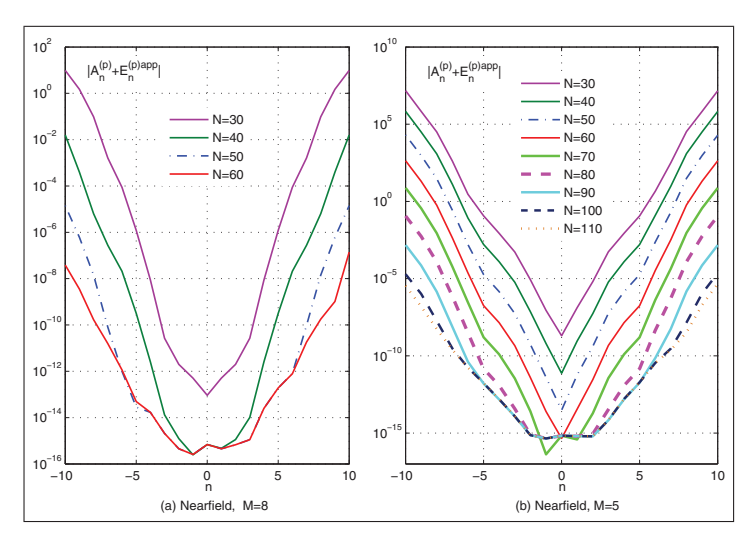


Figure 7. The near-field amplitude coefficients as a function of the Bessel function order n for different values of the truncation size N in equation (53) generated by (a) M=5 and (b) M=8 active sources, for longitudinal incidence.

The total power radiated by the sources is $\Sigma(\theta) = \Sigma^{(p)}(\theta) + \Sigma^{(s)}(\theta)$ where the compressional and shear far-field averaged radial flux vector components are

$$\Sigma^{(\alpha)}(\theta) = \int_0^{2\pi} d\theta |f_n^{(\alpha)}|^2 = 4 \sum_{n = -\infty}^{\infty} |F_n^{(\alpha)}|^2, \quad \alpha = p, s.$$
 (56)

The non-dimensional total scattering cross sections are then

$$Q = Q^{(p)} + Q^{(s)}$$
 where $Q^{(\alpha)} = \frac{4}{k_i a} \sum_{n=-\infty}^{\infty} |F_n^{(\alpha)}|^2$, $\alpha = p, s$. (57)

and $k_i = k_p$ for compressional incidence, $k_i = k_s$ for shear wave incidence. $Q^{(p)}$ and $Q^{(s)}$ are normalized by $a = a_1$, the radius of source A_1 , see Figure 1.

Results for the total scattering cross sections $Q^{(p)}$ and $Q^{(s)}$ for both longitudinal and transverse incidence are illustrated in Figure 8 versus the normalized wave number $k_i a$, and in Figure 9 against the number of active sources M. These show that the error increases with the rise of wave number k_i , but can be reduced by increasing M and N. The increase of N reduces the error sharply in all cases.

4.3. Total displacement field

4.3.1. Longitudinal plane wave incidence. First, consider longitudinal plane wave incidence of the form of equation (31). The total displacement vector components in Cartesian coordinates are

$$(u_x, u_y) = \left(\frac{\partial \Phi_i}{\partial x} + \frac{\partial \Phi_d}{\partial x} + \frac{\partial \Psi_d}{\partial y}, \frac{\partial \Phi_i}{\partial y} + \frac{\partial \Phi_d}{\partial y} - \frac{\partial \Psi_d}{\partial x}\right). \tag{58}$$

Introducing equations (31) and (6b) into equation (58) yields

$$\frac{u_{\mathbf{x}}}{k_{\mathbf{p}}} = \sum_{m=1}^{M} \sum_{n=-\infty}^{\infty} \left[B_{m,n}^{(\mathbf{p})} \left(\cos \theta_m V_n^{+\prime} \left(k_{\mathbf{p}} (\mathbf{x} - \mathbf{x}_m) \right) - i n \sin \theta_m \frac{V_n^{+\prime} \left(k_{\mathbf{p}} (\mathbf{x} - \mathbf{x}_m) \right)}{k_{\mathbf{p}} |\mathbf{x} - \mathbf{x}_m|} \right) + B_{m,n}^{(\mathbf{s})} \left(\kappa \sin \theta_m V_n^{+\prime} \left(k_{\mathbf{s}} (\mathbf{x} - \mathbf{x}_m) \right) + i n \cos \theta_m \frac{V_n^{+\prime} \left(k_{\mathbf{s}} (\mathbf{x} - \mathbf{x}_m) \right)}{k_{\mathbf{p}} |\mathbf{x} - \mathbf{x}_m|} \right) \right] + i \cos \psi_{\mathbf{p}} \Phi_i, \tag{59a}$$

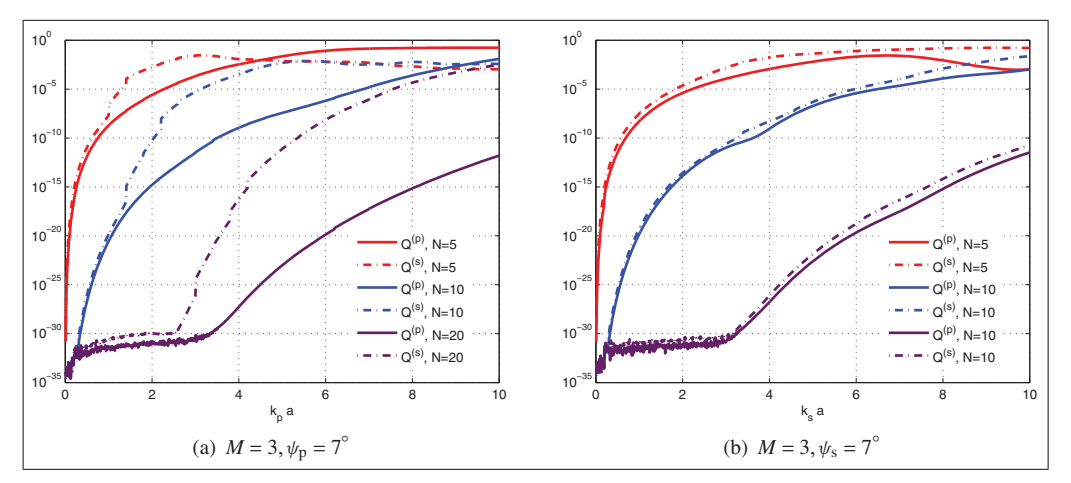


Figure 8. The total scattering cross sections $Q^{(p)}$ and $Q^{(s)}$ versus (a) the normalized wave number $k_p a$ for a longitudinal wave incidence, and (b) $k_S a$ for a transverse incidence.

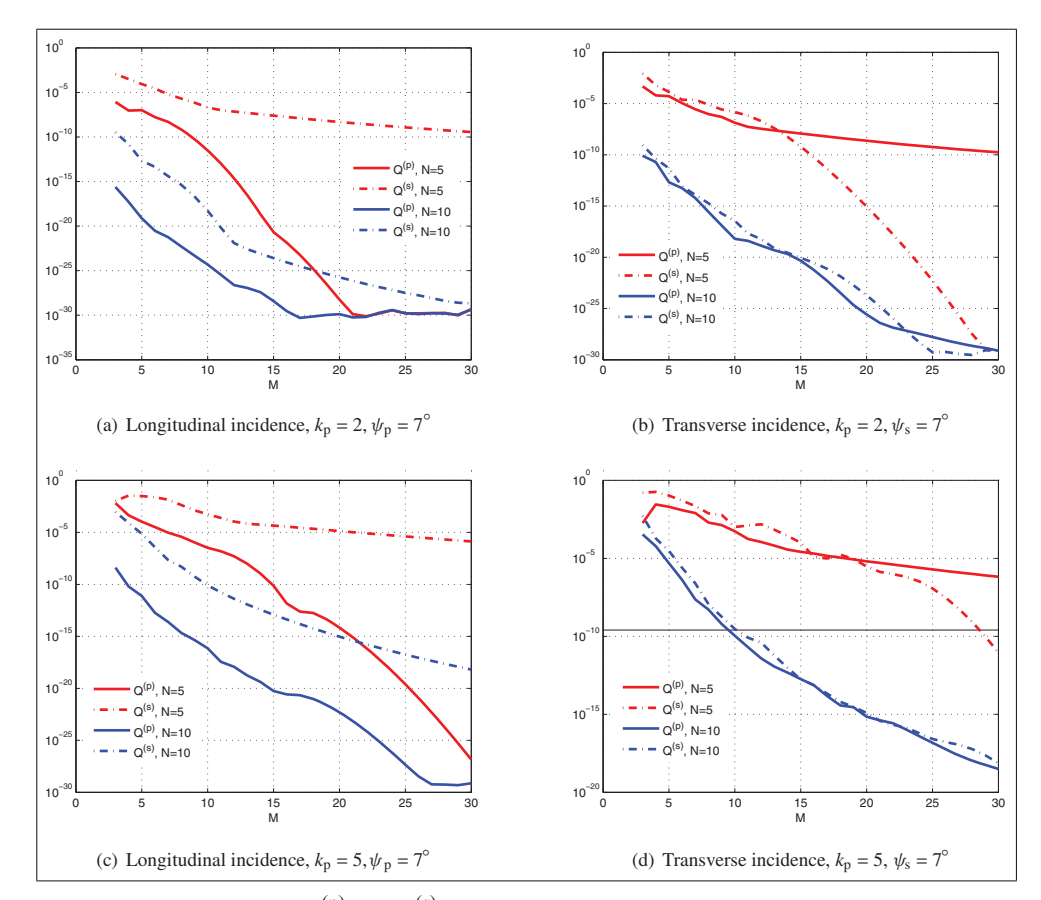


Figure 9. Total scattering cross sections $Q^{(p)}$ and $Q^{(s)}$ versus the number of active sources M for longitudinal ((a) and (c)), and transverse ((b) and (d)) wave incidence for $k_p=2$ and $k_p=5$ with $k_s=\kappa k_p$ and $\kappa=c_p/c_s$ when cloaking devices are ON.

$$\frac{u_{y}}{k_{p}} = \sum_{m=1}^{M} \sum_{n=-\infty}^{\infty} \left[B_{m,n}^{(p)} \left(\sin \theta_{m} V_{n}^{+'} \left(k_{p} (\mathbf{x} - \mathbf{x}_{m}) \right) + i n \cos \theta_{m} \frac{V_{n}^{+} \left(k_{p} (\mathbf{x} - \mathbf{x}_{m}) \right)}{k_{p} |\mathbf{x} - \mathbf{x}_{m}|} \right) + B_{m,n}^{(s)} \left(-\kappa \cos \theta_{m} V_{n}^{+'} \left(k_{s} (\mathbf{x} - \mathbf{x}_{m}) \right) + i n \sin \theta_{m} \frac{V_{n}^{+} \left(k_{s} (\mathbf{x} - \mathbf{x}_{m}) \right)}{k_{p} |\mathbf{x} - \mathbf{x}_{m}|} \right) \right] + i \sin \psi_{p} \Phi_{i},$$
(59a)

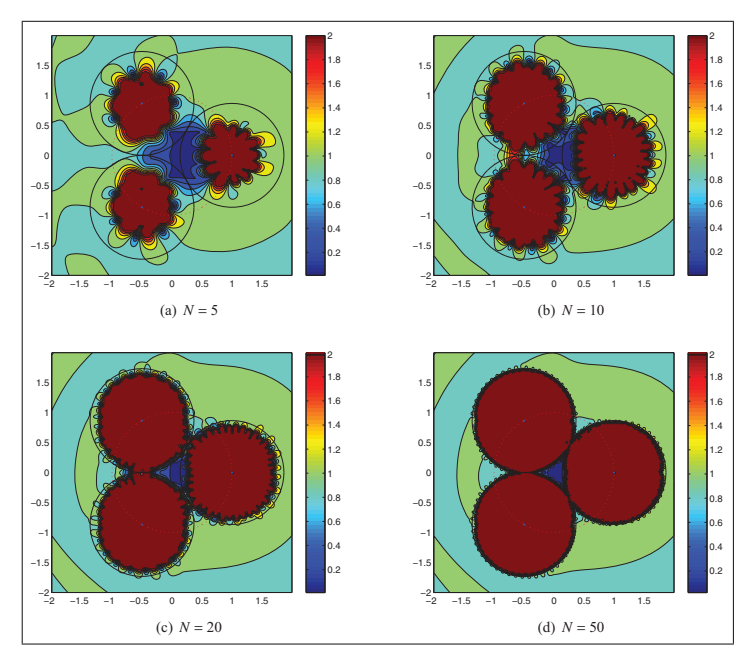


Figure 10. Absolute value of the displacement vector component $|u_x|/k_p$ for N=5 (a), N=10 (b), N=20 (c) and N=50 (d) when cloaking devices are active with $M=3, k_p=2$ for longitudinal wave incidence.

where

$$\theta_m(\mathbf{x}) = \arg(\mathbf{x} - \mathbf{x}_m). \tag{60}$$

4.3.2. Transverse plane wave incidence. Transverse incident plane waves are of the form of equation (40). The total displacement vector components in Cartesian coordinates are

$$(u_x, u_y) = \left(\frac{\partial \Phi_d}{\partial x} + \frac{\partial \Psi_i}{\partial y} + \frac{\partial \Psi_d}{\partial y}, \frac{\partial \Phi_d}{\partial y} - \frac{\partial \Psi_i}{\partial x} - \frac{\partial \Psi_d}{\partial x}\right). \tag{61}$$

Introducing equations (40) and (6b) into equation (61) yields

$$\frac{u_{x}}{k_{s}} = \sum_{m=1}^{M} \sum_{n=-\infty}^{\infty} \left[B_{m,n}^{(p)} \left(\kappa^{-1} \cos \theta_{m} V_{n}^{+'} \left(k_{p} (\mathbf{x} - \mathbf{x}_{m}) \right) - i n \sin \theta_{m} \frac{V_{n}^{+} \left(k_{p} (\mathbf{x} - \mathbf{x}_{m}) \right)}{k_{s} |\mathbf{x} - \mathbf{x}_{m}|} \right) \right. \\
+ \left. B_{m,n}^{(s)} \left(\sin \theta_{m} V_{n}^{+'} \left(k_{s} (\mathbf{x} - \mathbf{x}_{m}) \right) + i n \cos \theta_{m} \frac{V_{n}^{+} \left(k_{s} (\mathbf{x} - \mathbf{x}_{m}) \right)}{k_{s} |\mathbf{x} - \mathbf{x}_{m}|} \right) \right] + i \sin \psi_{s} \Psi_{i}, \tag{62a}$$

$$\frac{u_{y}}{k_{s}} = \sum_{m=1}^{M} \sum_{n=-\infty}^{\infty} \left[B_{m,n}^{(p)} \left(\kappa^{-1} \sin \theta_{m} V_{n}^{+'} \left(k_{p} (\mathbf{x} - \mathbf{x}_{m}) \right) + i n \cos \theta_{m} \frac{V_{n}^{+} \left(k_{p} (\mathbf{x} - \mathbf{x}_{m}) \right)}{k_{s} |\mathbf{x} - \mathbf{x}_{m}|} \right) \right. \\
+ \left. B_{m,n}^{(s)} \left(-\cos \theta_{m} V_{n}^{+'} \left(k_{s} (\mathbf{x} - \mathbf{x}_{m}) \right) + i n \sin \theta_{m} \frac{V_{n}^{+} \left(k_{s} (\mathbf{x} - \mathbf{x}_{m}) \right)}{k_{s} |\mathbf{x} - \mathbf{x}_{m}|} \right) \right] - i \cos \psi_{s} \Psi_{i}, \tag{62b}$$

where θ_m is defined by equation (60).

4.3.3. Results. The magnitude of the displacement vector components u_x and u_y are evaluated for $\psi_p = 7^\circ$ for various values of the truncation size N, the number of sources M, and the compressional wave number k_p . Greater accuracy is observed, as expected, with increased N and M. However, large N and M require longer computation time, and some numerical experimentation is necessary to find the smallest values for which the displacement field vanishes to the desired degree in the cloaked region.

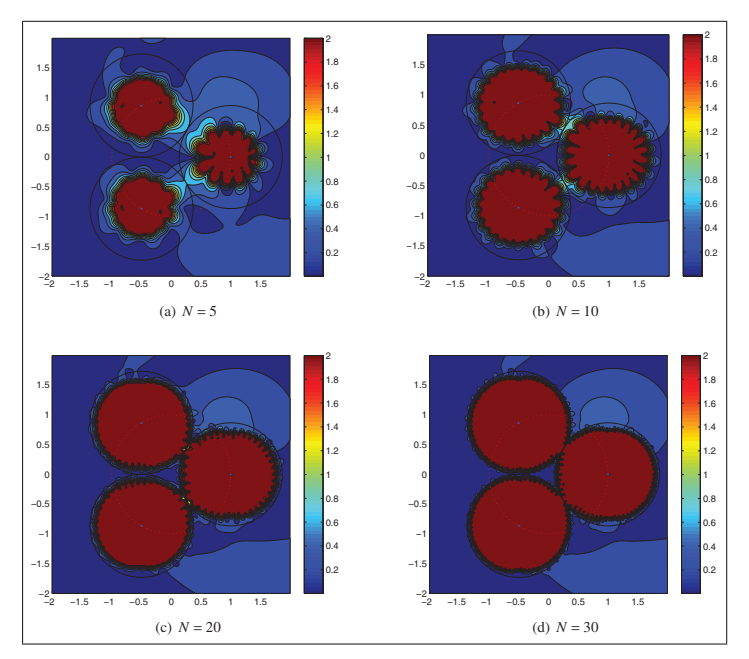


Figure 11. Absolute value of the displacement vector components $|u_y|/k_p$ for N=5 (a), N=10 (b), N=20 (c) and N=30 (d) when cloaking devices are active with $M=3, k_p=2$ for longitudinal wave incidence.

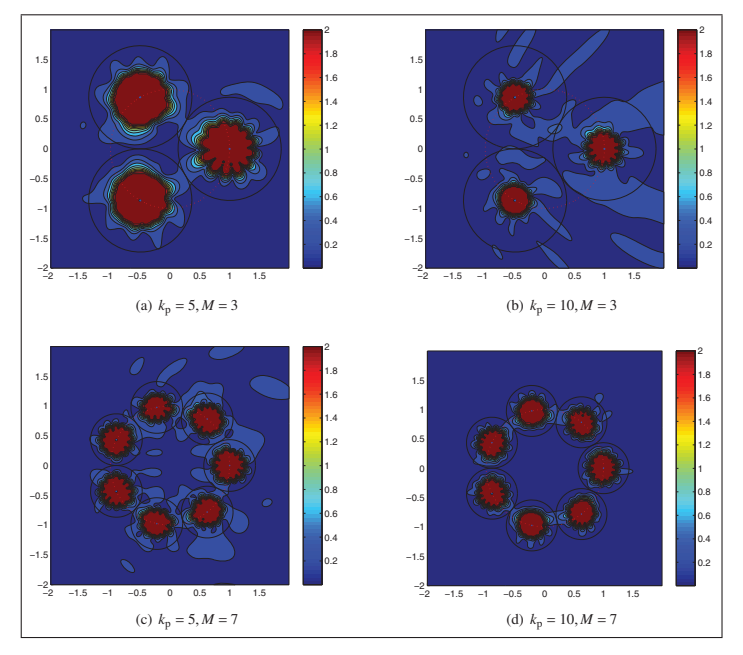


Figure 12. Absolute value of the displacement vector component $|u_y|/k_p$ for $k_p = 10, M = 3$ (a), $k_p = 10, M = 3$ (b), $k_p = 5, M = 7$ (c) and $k_p = 10, M = 7$ (d). Cloaking devices are active, N = 5, and longitudinal wave incidence.

The magnitudes of $|u_x|/k_p$ and $|u_y|/k_p$ are depicted in Figure 10 and Figure 11 for longitudinal incidence at different values of N when cloaking devices are active with $M=3, k_p=2$. As expected, the increase of N is accompanied by the reduction of magnitudes $|u_x|/k_p$ and $|u_y|/k_p$ in the cloaked region.

Figure 12 illustrates $|u_y|/k_p$ for longitudinal incidence with N=5 changing the values of k_p and M whilst Figure 13 and Figure 14 show corresponding values of $|u_x|/k_s$ and $|u_y|/k_s$ for shear incidence, varying N and M with $k_p=2$ for the former, and altering the values of N and k_p with M=3 for the latter. The magnitude of the total displacement field and its absolute maximum amplitude inside the cloaked region is depicted in Figure 15 with the parameters used in Figure 12. Comparison of these results shows that at higher frequencies, i.e., larger

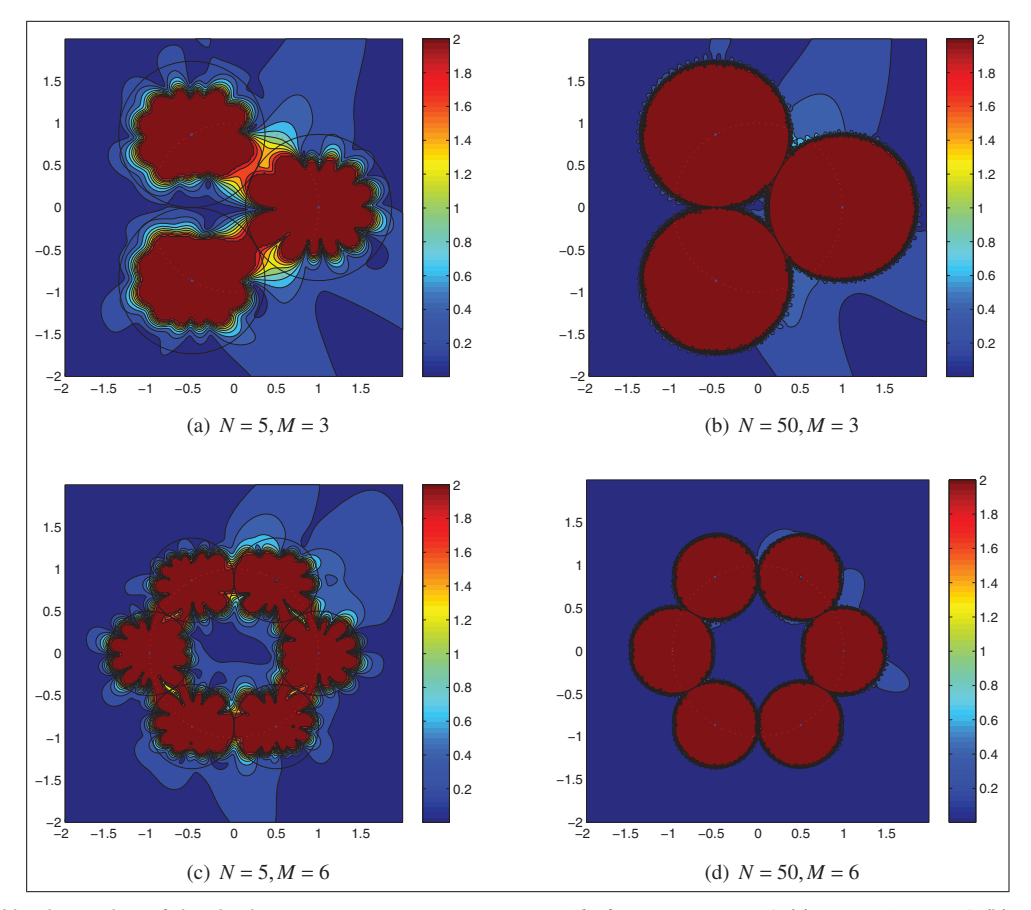


Figure 13. Absolute value of the displacement vector component $|u_x|/k_8$ for N=5, M=3 (a), N=50, M=3 (b), N=5, M=6 (c) and N=50, M=6 (d) when cloaking devices are active with $k_p=2, k_8=4.1305$ for transverse wave incidence.

values of k_p , greater accuracy is achieved by increasing the number of sources M, whereas at lower frequencies the smallest number of sources required, i.e. M=3, produces reasonable cloaking, although this is enhanced with increased values of N.

5. Conclusions

The external active acoustic cloaking model of Norris et al. [9] has been generalized to elastodynamics. Just as in the former case, it is possible to represent the sources in exact terms, although it requires that the incident elastic wave field is known in exact form; this is the price paid for active control. The control method proposed is based on representing the incident field in terms of regular functions (Bessel functions) at each source position, which leads to a linear system of equations for the source amplitudes that can be solved in closed form. The linear nature of the solution of this essentially inverse problem means that arbitrary incident wave motion can be treated by superposition.

The results presented here provide a first step in the direction of realistic active control of elastic waves. Applications to structure borne waves, surface waves, and even geophysical waves, are possible. However, as a *control* problem, many issues remain to be addressed. Not least is the issue of how to balance the goal of silencing one region of space with the unavoidable source noise that must be generated in another, larger, region. This quandary arises from the fact that the infinite series for the multipole expansion of the m active sources is divergent inside the domain A_m . Exact field cancellation is not achievable in practice; it becomes necessary to truncate the series and balance the decrease in cloaking accuracy with whatever amplitude level is deemed acceptable in the source region. This is obviously a crucial aspect and one that remains to be studied in detail. We have pointed out some similarities with parallel issues in active noise control, and future studies will examine analogies in these topics. One area for consideration is the low-frequency end of the spectrum. The numerical simulations presented here indicate that a small number of multipoles provide adequate cancellation

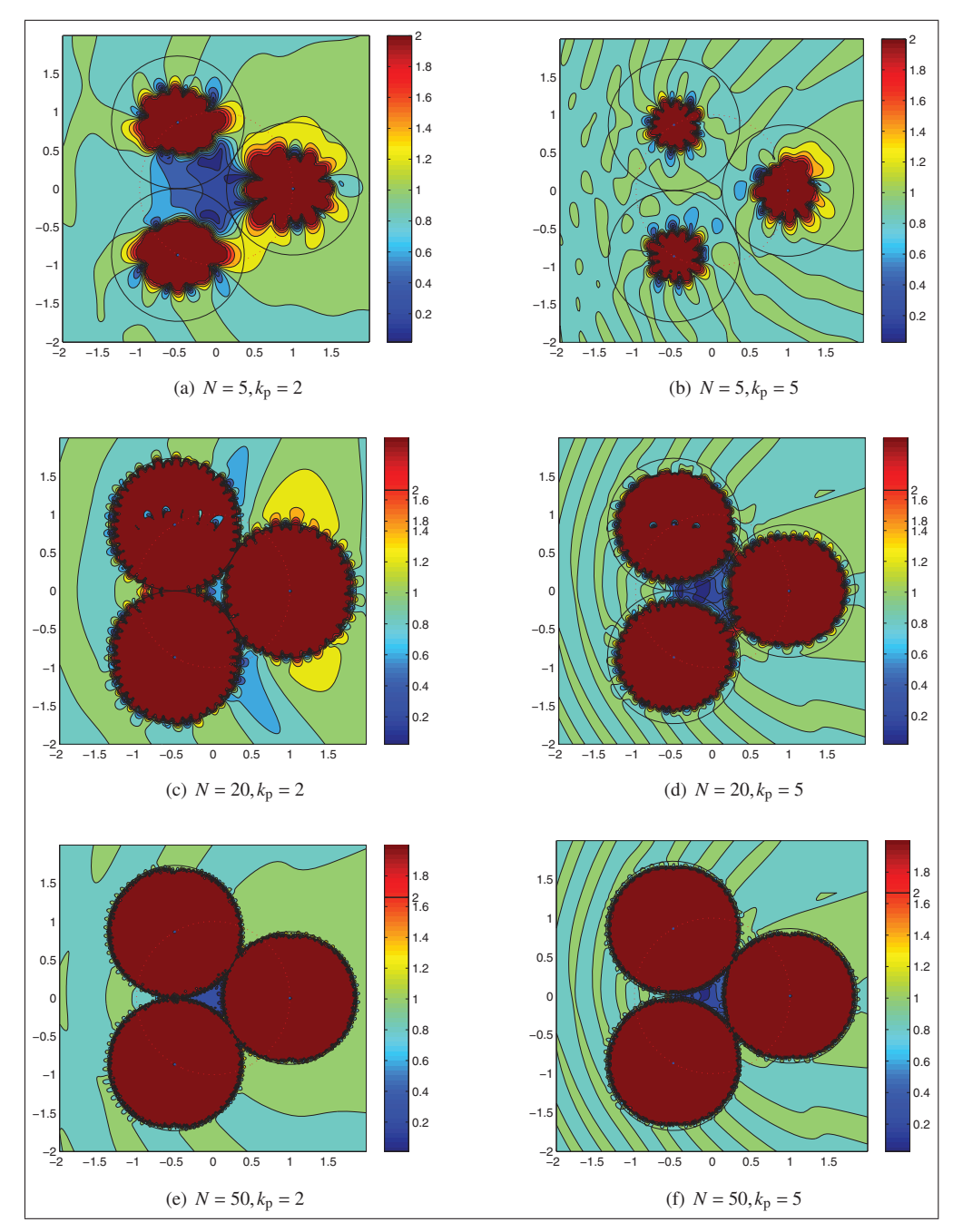


Figure 14. Absolute value of the displacement vector components $|u_y|/k_s$ for $N=5, k_p=2$ (a), $N=5, k_p=5$ (b), $N=20, k_p=2$ (c), $N=20, k_p=5$ (d), $N=50, k_p=2$ (f), and $N=50, k_p=5$ (e) with M=3 active sources for transverse wave incidence when the cloaking devices are active.

at low frequencies. This suggests a natural way to extend ideas based on monopoles to more elaborate source distributions composed of finite numbers of multipoles of low order. Hopefully, the present results provide a means to establish realistic strategies for practical application.

Funding

This work was supported by the ONR and the NSF.

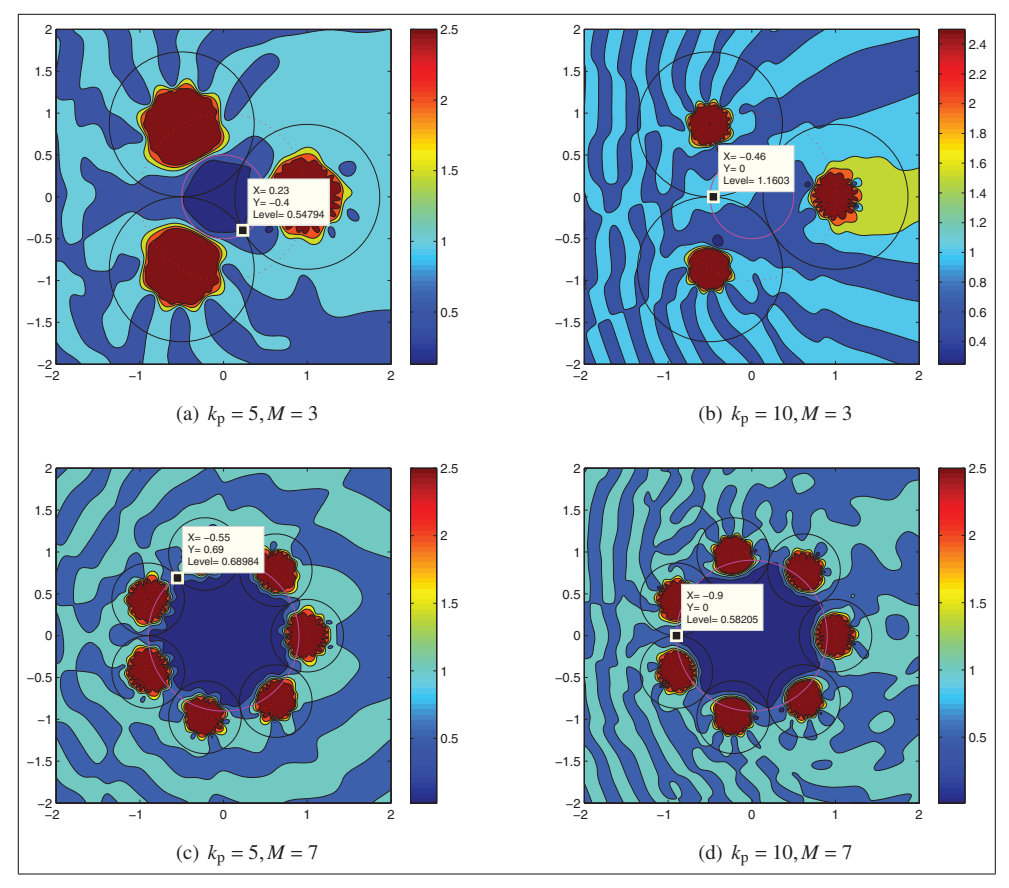


Figure 15. The magnitude of the total displacement field with its maximum absolute amplitude in a cloaked region generated by M=3 active sources with $k_p=5$ (a) and $k_p=10$ (b), and by M=7 active sources with $k_p=5$ (c) and $k_p=10$ (d) for a longitudinal wave incidence with $\psi_p=7^{\circ}$, N=5 while cloaking devices are active.

Conflict of interest

None declared.

References

- [1] Leonhardt, U. Optical conformal mapping. Science 2006; 312: 1777–1780.
- [2] Pendry, JB, Schurig, D, and Smith, DR. Controlling electromagnetic fields. Science 2006; 312: 1780–1782.
- [3] Cummer, SA, and Schurig, D. One path to acoustic cloaking. New J Phys 2007; 9: 45.
- [4] Miller, DA. On perfect cloaking. Opt Express 2006; 14: 12457–12466.
- [5] Vasquez, FG, Milton, GW, and Onofrei, D. Active exterior cloaking for the 2D Laplace and Helmholtz equations. Phys Rev Lett 2009; 103: 073901.
- [6] Vasquez, FG, Milton, GW, and Onofrei, D. Broadband exterior cloaking. Opt Express 2009; 17: 14800–14805.
- [7] Vasquez, FG, Milton, GW, Onofrei, D, and Seppecher, P. Transformation elastodynamics and active exterior acoustic cloaking. In: Guenneau, S, and Craster, R, (eds) *Acoustic metamaterials: negative refraction, imaging, lensing and cloaking*. Dordrecht: Springer, 2012.
- [8] Vasquez, FG, Milton, GW, and Onofrei, D. Exterior cloaking with active sources in two dimensional acoustics. Wave Motion 2011; 49: 515–524.
- [9] Norris, AN, Amirkulova, FA, and Parnell, WJ. Source amplitudes for active exterior cloaking. *Inverse Probl* 2012; 28: 105002.
- [10] Guicking, D. On the invention of active noise control by Paul Lueg. J Acoust Soc Am 1990; 87: 2251–2254.
- [11] Nelson, PA, and Elliott, SJ. Active control of sound. London: Academic Press, 1992.
- [12] McKinnell, RJ. Active vibration isolation by cancelling bending waves. Proc R Soc A 1989; 421: 357–393.
- [13] Fuller, CR, Elliott, SJ, and Nelson, PA. Active control of vibration. London: Academic Press, 1996.
- [14] David, A, and Elliott, SJ. Numerical studies of actively generated quiet zones. Appl Acoust 1994; 41: 63-79.
- [15] Kempton, AJ. The ambiguity of acoustic sources—A possibility for active control. J Sound Vib 1976; 48: 475–483.

[16] Milton, GW, Briane, M, and Willis, JR. On cloaking for elasticity and physical equations with a transformation invariant form. New J Phys 2006; 8: 248–267.

- [17] Brun, M, Guenneau, S, and Movchan, AB. Achieving control of in-plane elastic waves. Appl Phys Lett 2009; 94: 061903.
- [18] Norris, AN, and Shuvalov, AL. Elastic cloaking theory. Wave Motion 2011; 49: 525-538.
- [19] Parnell, WJ. Nonlinear pre-stress for cloaking from antiplane elastic waves. Proc R Soc A 2012; 468: 563–580.
- [20] Parnell, WJ, Norris, AN, and Shearer, T. Employing pre-stress to generate finite cloaks for antiplane elastic waves. Appl Phys Lett 2012; 100: 171907.
- [21] Norris, AN, and Parnell, WJ. Hyperelastic cloaking theory: Transformation elasticity with prestressed solids. *Proc R Soc A* 2012; 468: 2881–2903.
- [22] Abramowitz, M, and Stegun, I. *Handbook of mathematical functions with formulas, graphs, and mathematical tables*. New York: Dover, 1974.
- [23] Honarvar, F, and Sinclair, AN. Scattering of an obliquely incident plane wave from a circular clad rod. *J Acoust Soc Am* 1997; 102: 41–48.